DISCHARGE ESTIMATION IN A CHANNEL REACH RECEIVING SIGNIFICANT LATERAL INFLOW USING VPMS AND RCM METHODS

A DISSERTATION

Submitted in partial fulfilment of the

Requirements for the award of the degree of

MASTER OF TECHNOLOGY

in

HYDROLOGY

(With Specialization in Surface Water Hydrology)

By

NISHANT SAXENA

DEPARTMENT OF HYDROLOGY

INDIAN INSTITUTE OF TECHNOLOGY

ROORKEE-247667 (INDIA)

June, 2019

DECLARATION

I hereby declare that the work carried out in this Dissertation titled Discharge estimation in a channel reach receiving significant lateral inflow using VPMS and RCM methods is presented on behalf of partial fulfillment of the requirement for the award of degree of Master of Technology in Hydrology with specialization in Surface Water Hydrology, submitted to Department of Hydrology, Indian Institute of Technology, Roorkee, India, under the joint supervision of Professor Dr. Muthiah Perumal and Dr. Tommaso Moramarco.

I have not submitted the matter embodied in this report for the award of any other degree or diploma.

Date: 22/06/2019

Place: Roorkee, India

Nishant Saxena

(17537006)

CERTIFICATE

ABSTRACT

The conventional approach of discharge estimation involves the use of the *a-priori* developed rating curve at a gauging site, the development of which requires the use of measured river flow, against the corresponding observed water level or flow depth. This approach of developing rating curve often proves to be costly and tedious task. To circumvent this approach, Perumal et al. in 2007 and 2010 applied the Variable Parameter Muskingum Stage (VPMS) routing technique at those sites where only the stage measurements and channel characteristics are known. However, the approach did not involve the contribution of lateral flow from the intervening catchment of the considered river reach. In this study, an attempt is made to account for lateral flow contribution along the channel reach while routing using the VPMS method. Silvia et al. in 2017 applied the VPMS method accounting for lateral flow on a 50 km stretch of Tiber River in Central Italy and obtained reasonably acceptable results. This study is an extension of the same method with the only consideration of few constant wave travel times instead of using the travel times which were varying at every routing time interval. The appropriateness of using few wave travel times in the proposed method is also checked by conducting numerical experiments of its application by routing using the proposed method in hypothetical prismatic channel reaches. The routing solutions are compared with the benchmark solutions obtained using the well-known HEC-RAS model by routing the same input hydrograph in the same hypothetical channel reach considering the same lateral flow. Subsequently, both the approaches are compared for their application for the same flood events as used by Silvia et al. in 2017.

The Rating Curve Model(RCM) given by Moramarco et al. in 2005 is another technique to obtain the discharge information at a section where only the stage is monitored and discharge is recorded at an upstream section, and which also caters for the intervening catchment lateral inflow in the considered river reach. In this study, the application of the RCM model is tested for the same hypothetical channel section as is being used for testing the VPMS method. The RCM model used in this study involves the use of two ranges of wave travel time; the travel time being constant for the rising limb and varying with time in the recession limb. The method is also applied for different flood events of the Tiber River in a 50 km reach between the Santa Lucia and Ponte Felcino gauging stations and the results

obtained are compared with those obtained from the VPMS method. Finally, a comparative assessment is made for the applicability of both the methods in different flow situations.

Overall, this study reveals that the modified VPMS method considering a limited number of travel times while routing a flood wave scores better than the modified RCM method.

ACKNOWLEDGEMENT

I wish to express my sincere thanks to my supervisor Professor Muthiah Perumal for his guidance, inspiration, encouragement, pragmatic advice and unwavering support rendered to me throughout the completion of the project. His good teaching and in-depth knowledge with innovative ideas kept my curiosity and morale high.

I would also like to thank Dr. Tommaso Moramarco for providing useful inputs towards the improvement of my thesis work.

I am grateful to Dr. M.K Jain, Professor and Head, Department of Hydrology, IITR, for his generous help in providing the infrastructure during my Masters programme.

Heartfelt thanks to all the faculty of the Department of Hydrology, IITR for rendering their help and support.

I am extremely grateful to my colleague Mr. Kirtan Adhikari who helped me out in learning basics of computer programming. I am also thankful to my colleagues Mr. Aman Kumar Singh, Mr.Rajtosh Kr. Jha, Mr.Gurpinder Singh, and Mr.Ravi Meena who helped me to stay motivated during the course of my thesis work.

Immense gratitude to the huge community driven free and open source projects such as Python and NUMFOCUS. Analysis and figures were plotted using the products from NUMFOCUS.

Last but not the least, I would like to thank my parents who are always a constant source of support and inspiration to me. All those who have contributed directly or indirectly are highly acknowledged.

ABBREVIATIONS

Following symbols are used in this thesis

A	cross sectional area [L^2]
b	cross sectional bottom width [L]
c	wave celerity [LT^{-1}]
c_o	reference celerity corresponding to Q_o or y_o [LT^{-1}]
EVOL	percentage error in volume [-]
Fr	Froude number [-]
g	acceleration due to gravity [LT^{-2}]
I	Inflow Discharge [L^3T^{-1}]
m	exponent which depends upon frictional law (Manning's or Chezy's)
NSE	Nash-Sutcliff efficiency [%]
n	Manning's roughness coefficient [$TL^{-\frac{1}{3}}$]
P	wetted perimeter of the channel [L]
Q	Discharge [L^3T^{-1}]
Q^*	Attenuation in peak discharge[L^3T^{-1}]
q_L	Rate of lateral flow distribution[L^2T^{-1}]
R	hydraulic radius (A/P) [L]
S_o	channel bed slope [-]
S_f	frictional slope [-]
T	cross sectional top width [L]
T_L	Lag Time[T]
t	time [T]

T_P	time to peak [T]
v	velocity [LT^{-1}]
(v/g)(∂v/∂x)	convective acceleration gradient [-]
y	depth of water flow [L]
y_0	reference depth corresponding to Q_o [L]
y_M	maximum flow depth
∂y/∂x	longitudinal water surface gradient [-]
(1/g)(∂v/∂x)	local acceleration gradient [-]
(1/s_o)(∂y/∂x)	dimension-less longitudinal water surface gradient also applicability criterion for ACDW [-]
(1/s_o)(∂y/∂x)$_{max}$	maximum value of dimension-less longitudinal water surface gradient
Δt	computational time step [T]
γ	skewness factor of inflow hydrograph [-]
q_{per}	error in peak discharge [%]
y_{per}	error in peak velocity [%]
α, β	Model parameters of RCM

Table of Contents

LIST OF FIGURES

LIST OF TABLES

CHAPTER 1
INTRODUCTION

1.1 Background

Discharge assessment in rivers is one of the most important aspects in flood forecasting and management. The estimation of discharge hydrographs at a stream site is vital for planning and management of water resources in a region. However, the precise discharge estimation relies upon the channel properties at a gauging station. Local stage recording is quite straightforward and generally economically more viable, in contrast with the expenses incurred with both stream velocity estimations and topographic surveying of channel cross sections, particularly for locations with limited or unsuitable access. Hence, it is essential to convert stage records into discharge values through an accurate rating curve; in light of the previously mentioned reasons, the stage-discharge relationship may not be readily available at the desired sites in a river reach. In particular, velocity estimations are regularly available during low flow conditions ,so that the rating curve extrapolation for higher stages could be less reliable. Additionally, if there are unsteady flow conditions, an estimation of stage does not relate to a solitary estimation of discharge . This is indicated by a loop in the rating curve whose amplitude relies upon how much the inertial and pressure forces impact the flood movement(Moramarco and Singh, 2000). Thus, the usual practice of discharge estimation directly by using the rating curve of the gauging station may prove to be erroneous, especially, if the river bed slopes are flat.

To bypass the traditional procedures of stream discharge estimation, which are exorbitant, repetitive, and frequently hazardous during flood occasions, Perumal and Ranga Raju (1998) proposed the variable parameter Muskingum Stage Hydrograph (VPMS) routing technique for the calculation of discharge at an ungauged river site. This physically based simplified routing technique utilizes the data on (1) details of the two end cross sections of the river reach, (2) the average bed slope of the channel determined from the difference in elevations of the two end segments, (3) a set of upstream and downstream simultaneous stage hydrographs for adjusting the reach-averaged Manning's roughness coefficient, and (4) an equivalent prismatic channel section is fitted, approximately, between the upstream and downstream channel sections. It might be stressed that the VPMS routing technique utilizes the stage as the routing variable.

Another straightforward technique was proposed by Moramarco and Singh (2001) for reproducing the discharge hydrograph at a stream segment where just water level is observed and discharge is recorded at another upstream segment. This technique has two parameters connected to remotely observed discharge and without utilizing a flood routing system and without the need of a rating curve at a local site but by relating the stage at the gauging station with the hydraulic conditions at a remote upstream segment. The technique is known as the Rating Curve Model(RCM), as coined by Moramarco and Singh(2001).

Both the above discussed techniques, however, did not account for the significant lateral inflow along the considered reach in the development of the rating curve.

The Rating Curve Model (RCM), was upgraded by Moramarco et al. (2005) by including the portrayal of the lateral inflow that can happen along the selected river reach which obviously causes an increase in both the peak flow and the volume at the downstream section. The approach was checked for three reaches of the Upper-Middle Tiber River basin, in central Italy, with various attributes for both the drainage area and the branch itself (Moramarco et al., 2005). For whatever intermediate drainage area, without utilizing precipitation data, the model closely reproduced the hydrograph shape, the time to peak and the peak discharge of the few researched floods, certainly replicating the accessible rating curve in the downstream sections of the reaches considered. Recently, the usage of RCM has also extended to estimate the discharge along streams, even ineffectively gauged ones by exploiting water level estimates obtained using satellite altimetry(Tarpanelli et al., 2013).

Most of the simplified flood routing techniques also do not consider the presence of lateral flow along the routing reach. Such a non-consideration of lateral flow was addressed by Yadav et al. (2015) by considering uniform distribution of lateral flow along the reach and incorporating the same in the routing equation of the Variable-Parameter McCarthy-Muskingum (VPMM) technique(Perumal and Price, 2013), by utilizing a regression relationship between the total precipitation and runoff produced by excess rainfall of the intervening catchment. Afterwards,(Swain and Sahoo, 2015) considered the lateral flow in the VPMM technique considering non-uniform distribution of lateral flow along the length of the reach in direct proportion of the intervening sub-catchment area. Both these studies considered that the temporal distribution of lateral flow follows a similar pattern of the inflow hydrograph as considered by O'Donnell (1985) while applying the traditional Muskingum technique incorporating lateral flow. So as to improve the operational utility of the VPMM technique, both Yadav et al. (2015), and Swain and Sahoo (2015) set up the connection between the excess precipitation and the lateral flow, and the appropriateness of

this relationship relies upon the estimation of representative precipitation data and its spatial distribution over the intervening catchment of the considered routing reach of the river. The pre-requisite precipitation data might be hard to obtain, particularly in bumpy terrains where scanty or no-precipitation measurements are available.

In this study, the effect of lateral flow has been considered along the routing reach using the Variable Parameter Muskingum Stage routing method given by Perumal and Ranga Raju (1998). The routing technique, although did not consider the lateral flow component in its original formulation, has been modified to include the effect of lateral inflow using the method of characterisitcs approach. The routing technique using the VPMS method with significant lateral flow conditions was first investigated by Barbetta et.al.(2017). In this study, the same routing concept is used with the only modification that the parameter of wave travel time to be used in the VPMS method is considered constant unlike in the former approach where it was considered to be varying in space and every routing time interval. This consideration is in accordance with the kinematic nature of the rising limb of the inflow hydrograph with lateral flow component being added along the reach. Also, an improvement in the RCM method is being attempted in this study by taking into consideration more than one wave travel time, especially in case of gentle slopes. Both the methods are tested by using a hypothetical inflow hydrograph being routed in 25 different configurations of a prismatic trapezoidal channel section. The results are compared with respect to the benchmark outflow hydrographs obtained by using routing simulation of the same prismatic section using HEC-RAS model, after duly considering the uniform rate of lateral flow at any instant of time. The methods are also tested on a 50 km reach of the Tiber River(Central Italy). The results of the RCM and VPMS are compared together and a comparative analysis of the suitability of the two methods is presented.

1.2 Objectives

The basic objectives of this study are:

1. Application of the RCM and VPMS methods for hypothetical prismatic sections and by routing hypothetical hydrograph.
2. Verifying the theoretical basis of the modified RCM and VPMS methods by comparing with the benchmark solutions.
3. Field application of these methods to a selected reach of Tiber River in central Italy and simulating the observed stage and discharge hydrographs.

4. Comparing the two methods for their ability to do routing in the presence of significant lateral flow from the intervening catchment.

CHAPTER 2

LITERATURE REVIEW

2.1 General

2.2 The Saint Venant's Equations

The study of flood wave propagation in rivers is one of the most important facets in hydrology. The flood wave movement in rivers and channels is often governed by the use of basic equations which govern such flow processes. While going for surface runoff computations, river routing is a preferred option as it is less tedious than obtaining runoff and rainfall relationships.

The basic equations used in almost all the hydraulic routing techniques are the Saint Venant equations(Barrë de Saint-Venant,1871a,b), which consists of the hydraulic continuity and momentum equations. The Saint-Venant eqautions govern the one dimensional unsteady flow in rivers and channels.

$$\frac{\partial A}{\partial t} + \frac{\partial Q}{\partial x} = 0 \tag{2.1}$$

$$S_f = S_o - \frac{\partial y}{\partial x} - \frac{v}{g}\frac{\partial v}{\partial x} - \frac{1}{g}\frac{\partial v}{\partial t} \tag{2.2}$$

where, t= time; x= distance along the channel; y= flow depth; v= average cross-sectional velocity; A = cross-sectional area; Q= discharge; g= acceleration due to gravity;

S_f= frictional slope; S_0= bed slope; $\partial y/\partial x$= longitudinal gradient of water profile;

$\frac{v}{g}\ \partial v/\partial x$= convective acceleration slope; $1/g\ \ \partial v/\partial t$= local acceleration slope. Equation (3.1) represents the continuity equation, and Equation (3.2) represents the momentum equation. The routing techniques involving the use of the full Saint Venant's equations are called hydraulic routing techniques.

Most of the modelling packages available such as HEC-RAS(USACE) and MIKE-11(DHI) use the numerical solutions of the Saint-Venant eqautions for routing purposes. The numerical solution of the Saint-Venant equations using explicit and implicit scheme of the finite difference technique has also been proposed, which is beyond the scope of this study.

2.3 The Muskingum Method

McCarthy in 1938 proposed a hydrological routing procedure in which outflow discharge in a finite river reach is solved directly as a function of inflow discharge, in which all the morphological and hydraulic properties are lumped into a number of model parameters.

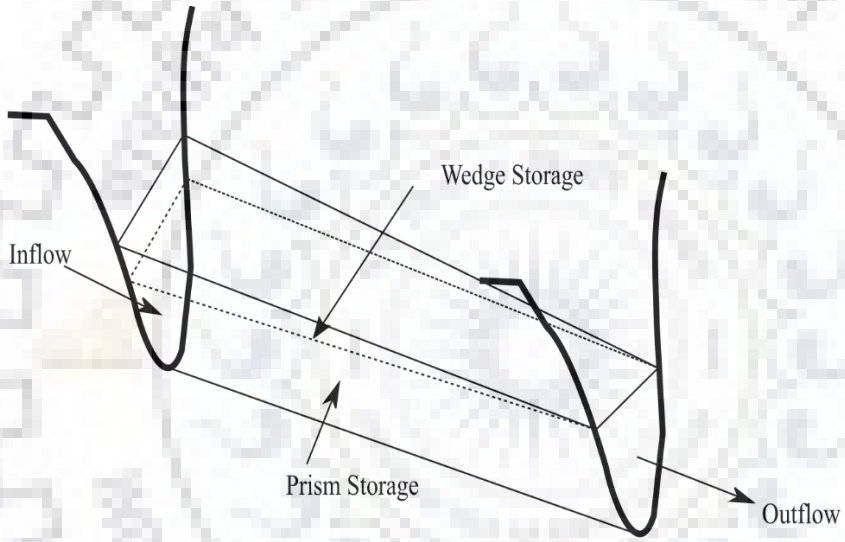

Figure 2-1 The prism and wedge storage

The total storage was considered to be composed of two parts:

1. Prism storage
2. Wedge storage

The prism storage refers to the volume that would exist if the uniform flow occurred at the downstream depth. The wedge storage refers to the wedgelike volume formed between the actual water surface profile and the top surface of the prism storage. For a particular depth, the prism storage remains constant, whereas the wedge storage varies from a positive value during the rising stage of flood and to a negative value during a receding flood.

The total storage in a channel reach can be expressed as

$$S = K[xI^m + (1-x)Q^m \quad (2.3)$$

where, K represents wave travel time and x is the weighing factor. The value of x generally lies within 0 and 0.5.

The above equation when combined with the lumped continuity equation,i.e.,

$$I - Q = \frac{dS}{dt} \quad (2.4)$$

gives the following expression for outflow discharge, which is also the governing equation for channel routing

$$Q_2 = C_o I_2 + C_1 I_1 + C_2 Q_1 \quad (2.5)$$

where

$$C_o = \frac{-Kx+0.5\Delta t}{K-Kx+0.5\Delta t} \quad (2.5A)$$

$$C_1 = \frac{Kx+0.5\Delta t}{K-Kx+0.5\Delta t} \quad (2.5B)$$

$$C_2 = \frac{K-Kx+0.5\Delta t}{K-Kx+0.5\Delta t} \quad (2.5C)$$

Q and I refer to outflow and inflow hydrographs respectively. Suffixes 1 and 2 refer to flow conditions before and after the time interval Δt.

2.4 The VPMS method

The hydraulic approach of flood routing is a preferred choice over the hydrological semi-empirical approaches as the former approach requires only the information of channel geometry and flow resistance characteristics at closer spatial intervals, and has the ability to produce both stage and discharge output simultaneously at the gauging station itself as well as of the intermediate gauging stations. But, obtaining the discharge information as well as the channel geometry at closer intervals over the long reach involved is not always feasible.

Moreover, the use of software packages such as HEC-RAS(USACE,2008) and MIKE11(DHI-*Water and Environment*,2008) is not always viable due to their inherent limitation of requirement of cross-section details and roughness information at closer intervals. For developing countries, this factor is of all the more prominence due to their limited data and computing resources. Thus, the less data intensive simplified flood routing techniques can be used in practical field applications.

One of the simplified routing techniques used in this study is the variable parameter Muskingum Stage routing method(Perumal and Ranga Raju,1998),also known as the VPMS method, which uses only stage at the inflow section as input, and is able to produce stage as well as discharge hydrographs at the outflow section simultaneously. The idea behind development of this method is that usually the flood routing is carried out by converting measured stage into discharge using a steady-state rating curve. While such a routing technique may be useful for steady flow, in case of unsteady flow, there will be a looped rating curve, in which case we will have two discharge values for a particular stage value, thus discharge estimation by using the rating curve technique in such a case may prove to be erroneous. Also, continuous stage measurement is more feasible and economical than continuous discharge measurement.

Keeping these points in consideration, a variable parameter Muskingum type method for stage hydrograph routing was developed directly from the Saint-Venant's equations. The form of the routing equation remains the same, except that the discharge term is replaced by the stage term.

2.4.1 Assumptions:

1. A prismatic section having any shape of cross-section (Rectangular, Trapezoidal, Triangular) is considered.

2. The water surface slope ($\frac{\partial y}{\partial x}$), the local acceleration term ($\frac{1}{g}\ \frac{\partial v}{\partial t}$), and convective acceleration term ($\frac{v}{g}\ \frac{\partial v}{\partial x}$) are small, but not negligible.

3. Lateral flow is not considered along the reach.

4. At any instant of time, during unsteady flow, there exists a one-to-one steady flow relationship between the flow depth at the mid-section of the reach and the discharge passing somewhere downstream of it. This assumption is also used in the Kalinin-Milyukov method(Appolov et al.1964).

2.4.2 Development of method:

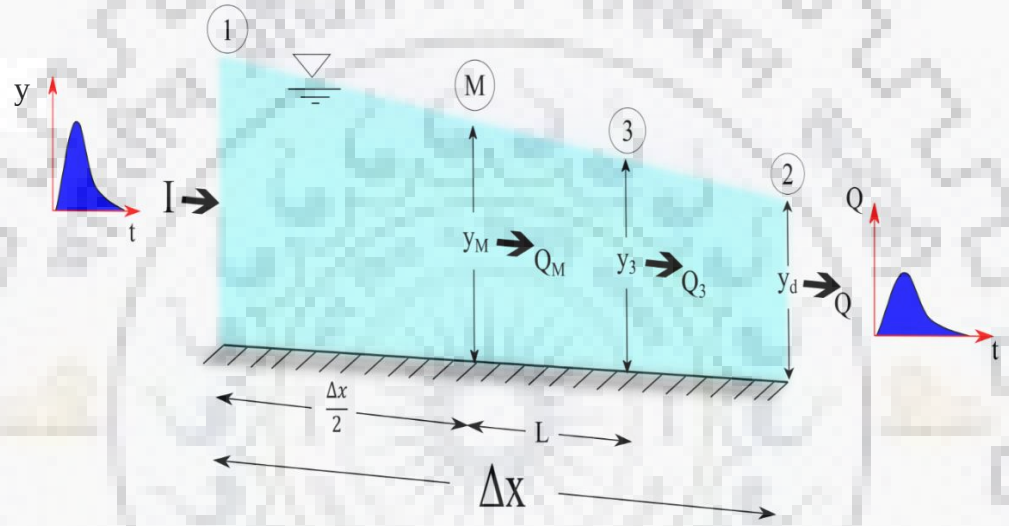

Figure 2-2 VPMS routing reach schematic

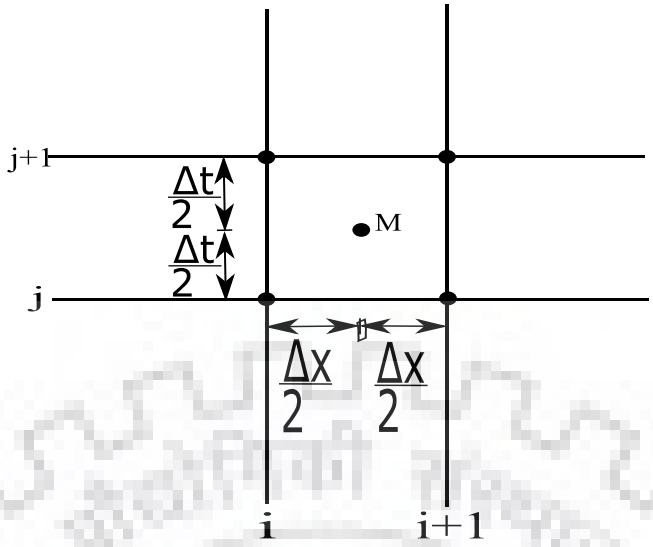

Figure 2-3 Computational grid of VPMS

In the development of the VPMS method(Perumal, Moramarco, Sahoo, & Barbetta, 2007), the governing Approximate Convection-Diffusion(ACD) equation in stage form was applied at section 3 of the reach at j^{th} time level of the computational grid as shown in figure (3-2). Subsequently, the recursive Muskingum-type routing equation was developed. The routing parameters k and θ were obtained using the location of y_3 from the mid-section and the celerity of flow at section 3, both corresponding to the j^{th} time level, which is erroneous. The conventional form of the VPMS method did not account for the variation in the value of celerity at j^{th} and $(j-1)^{th}$ time level.

The above error was corrected by Mohanty and Perumal by applying the ACD equation at the mid-point M of the box-grid located at the coordinate$(\frac{\Delta x}{2}, \frac{\Delta t}{2})$,as shown in figure(3-2) ,and by appropriately considering the location of section 3 and the velocity of flow at this section corresponding to mid-time level of the box-grid scheme.

The routing equation was developed as a simplified solution of the Saint Venant equations by applying the hydraulic continuity equation at the centre of the box-grid scheme, with the grid space length denoting the Muskingum reach length Δx and the top and bottom of these horizontal grid space lengths defining the current and the previous computational time level Δt, respectively.

The hydraulic continuity equation applied at the centre of the grid is expressed as

$$\frac{\partial A_M}{\partial t} + \frac{\partial Q_M}{\partial x} = 0 \tag{2.6}$$

where, A_M and Q_M are the cross-sectional area and discharge at the midpoint of the grid, respectively.

Neglecting inertial terms, the discharge Q_M can be expressed as (Henderson,1966)

$$Q_M = Q_{M0}\left(1 - \frac{1}{S_0}\frac{\partial y}{\partial x}\right)^{\frac{1}{2}} \tag{2.7}$$

where, Q_{M0} is the steady flow discharge corresponding to flow depth y_M at the centre of the grid. As per the earlier assumption, the steady discharge Q_{M0} , denoted as Q_3, passes at section 3 of Figure(3-1) during the unsteady flow. Accordingly,

$$Q_M = Q_3\left(1 - \frac{1}{S_0}\frac{\partial y}{\partial x}\right)^{\frac{1}{2}} \tag{2.8}$$

or,
$$Q_3 = Q_M\left(1 - \frac{1}{S_0}\frac{\partial y}{\partial x}\right)^{-\frac{1}{2}} \tag{2.9}$$

Expanding equation (3.9) can be expanded using the binomial series considering $\left|\frac{1}{S_0}\frac{\partial y}{\partial x}\right|_M \ll 1$, and neglecting higher order terms,

$$Q_3 = Q_M + \frac{Q_M}{2S_0}\left|\frac{\partial y}{\partial x}\right|_M \tag{2.10}$$

$\left|\frac{\partial y}{\partial x}\right|_M$ can be expressed as(Perumal, 1994)

$$\left|\frac{\partial y}{\partial x}\right|_M = \frac{1}{B_M c_M}\left(\frac{\partial Q}{\partial x}\right)_M \tag{2.11}$$

where, B_M and c_M are the topwidth and celerity of flow at mid-section, respectively. Therefore, equation (2.10) becomes

$$Q_3 = Q_M + \frac{Q_M}{2S_0 B_M c_M}\left|\frac{\partial Q}{\partial x}\right|_M \tag{2.12}$$

From equation (2.12), it can be inferred that the section 3 , where the discharge Q_3 passes, is located at a distance $\frac{Q_M}{2S_0 B_M c_M}$ from the mid-section M.

Applying continuity equation at section 3,

$$\frac{\partial A_3}{\partial t} + \frac{\partial Q_3}{\partial x} = 0 \tag{2.13}$$

$$\frac{dA_3}{dy} c_3 \frac{\partial y_3}{\partial x} + \frac{\partial A_3}{\partial y}\frac{\partial y_3}{\partial t} = 0 \tag{2.14}$$

$$\frac{\partial y_3}{\partial t} + c_3 \frac{\partial y_3}{\partial x} = 0 \tag{2.15}$$

Equation (3.15) is the governing ACD equation of the IVPMS method applicable at $\frac{\Delta t}{2}$ time level of the grid.

Assuming the linear variation of stage over the Muskingum reach,

$$\frac{\partial y_3}{\partial x} = \frac{\partial y_M}{\partial x} \tag{2.16}$$

or, $$\frac{y_3 - y_M}{l} = \frac{\partial y_M}{\partial x} \tag{2.17}$$

where, l is the distance between the mid-section and section 3, and, $y_M = \frac{y_d + y_u}{2}$,

Thus,

$$y_3 = y_M + l\frac{\partial y_M}{\partial x} \tag{2.18}$$

Using equation (2.18) in equation (2.15),

$$\frac{\partial}{\partial t}\left(y_M + l\frac{\partial y_M}{\partial x}\right) + c_3\frac{\partial y_M}{\partial x} = 0 \tag{2.19}$$

Applying central finite difference scheme in equation (2.19),

$$\frac{\left(y_M + l_{av}\frac{\partial y_M}{\partial x}\right)_j - \left(y_M + l_{av}\frac{\partial y_M}{\partial x}\right)_{j-1}}{2\frac{\Delta t}{2}} + c_{3av}\frac{1}{2}\left[\left.\frac{\partial y_M}{\partial x}\right|_j + \left.\frac{\partial y_M}{\partial x}\right|_{j-1}\right] = 0 \tag{2.20}$$

where,

$$l_{av} = \frac{l_j + l_{j-1}}{2} \; and \; c_{3av} = \frac{c_{3,j} + c_{3,j-1}}{2} \tag{2.21}$$

Further simplification leads to

$$\frac{y_{M,j} + \frac{l_{av}(y_{d,j} - y_{u,j})}{2\frac{\Delta x}{2}} - y_{M,j-1} - \frac{l_{av}(y_{d,j-1} - y_{u,j-1})}{2\frac{\Delta x}{2}}}{2\frac{\Delta t}{2}} + c_{3av}\frac{1}{2}\left[\frac{(y_{d,j} - y_{u,j})}{2\frac{\Delta x}{2}} + \frac{(y_{d,j-1} - y_{u,j-1})}{2\frac{\Delta x}{2}}\right] \tag{2.22}$$

By separating the known and unknown variables, the routing equation of the IVPMS method is obtained as

$$y_{d,j} = C_1 y_{u,j} + C_2 y_{u,j-1} + C_3 y_{d,j-1} \tag{2.23}$$

where,

$$C_1 = \frac{-K\theta+0.5\Delta t}{K(1-\theta)+0.5\Delta t} \quad (2.23A)$$

$$C_2 = \frac{K\theta+0.5\Delta t}{K(1-\theta)+0.5\Delta t} \quad (2.23B)$$

$$C_3 = \frac{K(1-\theta)-0.5\Delta t}{K(1-\theta)+0.5\Delta t} \quad (2.23C)$$

The parameter K denotes the wave travel time and θ denotes the weighing parameter, and are expressed as

$$K = \frac{\Delta x}{c_{3av}} \quad (2.24)$$

$$\theta = \frac{1}{2} - \frac{1}{4S_0\Delta x}\left(\frac{Q_{3,j}}{B_{M0,j}c_{M0,j}} + \frac{Q_{3,j-1}}{B_{M0,j-1}c_{M0,j-1}}\right) \quad (2.25)$$

2.4.3 VPMS method with lateral flow consideration:

The lateral flow in a river reach can be considered as a direct contribution of the surface runoff from the intervening catchment through which the channel passes. One of the ways of accounting the lateral flow contribution is to develop a rainfall-runoff relationship as adopted by Yadav el al. (2015). However, such a process is data intensive and involves tedious rainfall computations.

In the present study, the lateral flow component has been considered similar to the one given by O'donnell (1985) which assumed that the rate of lateral inflow along the reach and rate of entrance of inflow into the reach bear a proportional relationship. Thus, the lateral

flow hydrograph q_L is distributed uniformly along the length of the reach at any instant of time during the passage of flood wave in the concerned reach length at any time during the passage of flood wave in the study reach.

Keeping the above points in mind, the continuity equation considering the effect of lateral flow can be expressed as

$$\frac{\partial A}{\partial t} + \frac{\partial Q}{\partial x} = q_L \tag{2.26}$$

Applying equation (2.26) at section 3 of the VPMS routing reach,

$$\frac{\partial y_3}{\partial t} + \frac{\partial Q_3}{\partial A}\frac{dA}{dy}\Big|_3 \frac{\partial y_3}{\partial x} = q_L \tag{2.27}$$

or,

$$\frac{\partial y_3}{\partial t} + \frac{\partial Q_3}{\partial A}\frac{dA}{dy}\Big|_3 \frac{\partial y_3}{\partial x} = q_L$$

or,

$$\frac{\partial y_3}{\partial t} + c_3 \frac{\partial y_3}{\partial x} = \frac{q_L}{B_3} \tag{2.28}$$

Using the assumption of linear variation of stage and substituting $y_3 = y_M + \frac{Q_{M0}}{2S_0 B_M c_{M0}}\frac{\partial y_M}{\partial x}$,

where, y_M is the mid-section depth and Q_{M0} denotes the normal discharge corresponding to depth y_M, the following expression can be obtained

$$\frac{\partial}{\partial t}\left(y_M + \frac{Q_{M0}}{2S_0 B_M c_{M0}}\frac{\partial y_M}{\partial x}\right) + c_3 \frac{\partial y_3}{\partial x} = \frac{q_L}{B_3} \tag{2.29}$$

Applying equation (2.29) at the centre point of the computational grid, and further simplifying it, the following routing equation of IVPMS can be obtained

$$y_{i+1,j+1} = C_1 y_{i,j+1} + C_2 y_{i,j} + C_3 y_{i+1,j} + C_4\left[\left(\frac{q_L}{B_3}\right)_{i+1,j+1} + \left(\frac{q_L}{B_3}\right)_{i+1,j}\right] \tag{2.30}$$

Coefficients C_1, C_2 and C_3 are the same as used in equation (3.23) while coefficient C_4 can be expressed as

$$C_4 = \frac{0.5K\Delta t}{K(1-\theta)+0.5\Delta t} \tag{2.31}$$

2.4.4 Assessment of lateral flow contribution:

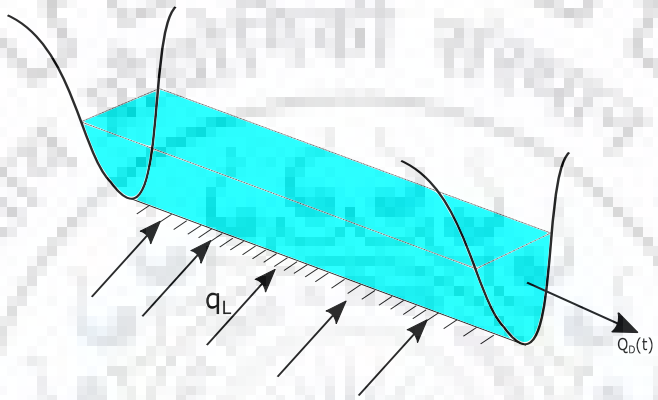

Figure 2-4 Lateral flow representation along the river reach

From the continuity equation, we have

$$\frac{\partial A}{\partial t} + \frac{\partial Q}{\partial x} = q_L \tag{2.32}$$

It can also be written as

$$\frac{\partial Q}{\partial A}\frac{\partial A}{\partial x} + \frac{\partial A}{\partial t} = q_L \tag{2.33}$$

or,

$$\frac{dA}{dt} = q_L \tag{2.34}$$

which is the continuity equation in characteristic form(Moramarco et al., 2005)

The above equation is applicable for the characteristic path defined by $\frac{dx}{dt} = c = \frac{\partial Q}{\partial A}$,

c being the kinematic celerity of the flood wave. Assming that T_L is the time required to match the upstream and downstream dimensionless stage hydrographs, the value of c is taken as $c = \frac{L_{reach}}{T_L}$. The dimensionless stage hydrographs are obtained by

$$h^*(t) = \frac{h(t)-h_b}{h_p-h_b} \tag{2.35}$$

where, $h(t)$ is the stage at any time t, h_b and h_p are the minimum and maximum values of the stage hydrograph observed, respectively. Thus, the lateral flow rate is estimated by

$$\frac{A_d(t)-A_u(t-T_L)}{T_L} = q_L \tag{2.36}$$

where, A_d represents the downstream flow area and A_u represents the upstream flow area of the reach under consideration.

2.5 The Rating Curve Model

The rating curve model is another technique is another method for discharge estimation when there are significant lateral inflows along the reach. It was first developed by Moramarco and Singh(2001) as a discharge estimation technique at a site where only stage is recorded, and discharge is recorded at another section upstreram. Later, it was enhanced by Moramarco et al.(2005) to incorporate significant lateral inflows. The model is not a flood routing procedure and allows a quick estimation of outflow discharge through the computation of two parameters which are linked to the discharge values recorded at a section some distance away.

2.5.1 Development of method:

The basic equation for computing outflow discharge in a river reach, where the stage and the surveyed stage-area relation are given at the two ends, and the discharge is known at the upstream section, while receiving significant lateral inflows is

$$Q_D(t) = \alpha \frac{A_D(t)}{A_U(t-T_L)} Q_U(t - T_L) + \beta \quad (2.37)$$

where, Q_U is the upstream discharge, A_D and A_U are the downstream and upstream flow areas respectively, T_L is the wave travel time, and α and β are model paramters.

Equation (3.37) is based on Chiu's entropy formulation(Chiu,1991), which stated that the mean flow velocity at a section is a function of the maximum velocity through a dimensionless parameter M.

$$\bar{u} = \Phi(M) u_{max} \quad (2.38)$$

where, $$\Phi(M) = \left(\frac{e^M}{e^M - 1} - \frac{1}{M}\right) \quad (2.39)$$

On application of the above equations over several gauging stations (Moramarco et al.2004, Xia(1997)), it was found that for a wide range of flow conditions, the value of $\Phi(M)$ was constant and time invariant (Chiu and Tung(2002)).

The above findings lead to the conclusion that there exists a direct one-to-one relationship between upstream and downstream velocities, and that lead to the following proportionality equation

$$Q_D(t) = \alpha \frac{A_D(t)}{A_U(t)} Q_U(t) \quad (2.40)$$

The above equation was modified by Moramarco et al.(2005) to give equation (2.37) which made it suitable to account for significant lateral inflow.

2.5.2 Parameter estimation:

The parameters α and β are estimated as

$$\alpha = \frac{\boldsymbol{Q_D}(T_P) - \boldsymbol{Q_D}(T_B)}{\left[\frac{A_D(T_P)}{A_U(T_P - T_L)} Q_U(T_P - T_L) - \frac{A_D(T_B)}{A_U(T_B - T_L)} Q_U(T_B - T_L)\right]} \quad (2.41)$$

$$\beta = Q_D(T_B) - \alpha \frac{A_D(T_B)}{A_U(T_B - T_L)} Q_U(T_B - T_L) \quad (2.42)$$

where, T_B is the time when baseflow occurs and T_P is the time of occurrence of peak stage at the downstream section.

2.5.3 Computation of Baseflow:

The baseflow contribution can be computed either by carrying out wading measurements or, by assuming constant mean velocity between the upstream and downstream sections, the baseflow $Q_D(T_B)$ can be computed as the product of the upstream mean velocity and the downstream flow area, i.e.,

$$Q_D(T_B) = \frac{Q_U(T_B - T_L)}{A_U(T_B - T_L)} A_D(T_B) \quad (2.43)$$

2.5.4 Downstream Peak Discharge Computation:

The downstream peak discharge computation is composed of calculation of two terms: the upstream peak discharge lagged by time T_L,i.e., $Q_U(T_P - T_L)$ with its attenuation due to routing along the reach, and the contribution of lateral flow along the reach, $q_P L$.

$$Q_D(T_P) = Q_U(T_P - T_L) - Q^* + q_P L \quad (2.44)$$

The term Q^* denotes the attenuation in peak discharge(Price, 1974) and is given by

$$Q^* = \frac{K}{(\frac{L}{T_L})^3} \times Q_U(T_P) \times \left| \frac{Q_1 + Q_{-1} - 2Q_U(T_P)}{(\Delta t^*)^2} \right| \quad (2.45)$$

where, K=$\frac{L}{2BS_0}$; B and S_0 being the mean channel width and bed slope, respectively, $Q_U(T_P)$= upstream peak discharge, Q_1 and Q_{-1} are discharge values at time Δt^* to the either side of the peak of the upstream discharge hydrograph, and Δt^* is one-fifth of the time to peak of the upstream discharge hydrograph

2.5.5 Computation of lateral flow contribution:

The lateral flow component is computed by using the characteristic form of the continuity equation as discussed earlier, i.e.,

$$\frac{dA}{dt} = q_P \tag{2.46}$$

or, $$\frac{A_D(T_P) - A_U(T - T_L)}{T_L} = q_P \tag{2.47}$$

where, A_D and A_U are the downstream and upstream flow areas, respectively, q_P is the rate of addition of lateral flow, and T_L is the time lag necessary to match the rising limb of the upstream and downstream dimensionless stage hydrographs.

2.6 Performance Evaluation Criteria

The results obtained using both the methods, i.e., the VPMS and the RCM method, are verified using the performance evaluation criteria given by Perumal & Sahoo (2007). The routed hydrographs obtained by the application of these methods on the hypothetical channel section as well as on the field data are compared with the observed ones by using the Nash-Sutcliffe efficiency(NSE) for both stage and discharge hydrograph reproduction, the Percentage error in peak discharge Q_{per} and peak stagey_{per} , and the percentage error in volume(EVOL).

2.6.1 The Nash-Sutcliffe Efficiency

$$NSE = \left(1 - \frac{\sum_{i=1}^{N}(Q_{obsi} - Q_{simi})^2}{\sum_{i=1}^{N}(Q_{obsi} - \overline{Q_{obs}})^2}\right) \times 100 \tag{2.48}$$

2.6.2 Percentage Error in the Peak

$$y_{per} = \left(\frac{y_{pcomp}}{ypbm} - 1\right) \times 100 \tag{2.49}$$

$$q_{per} = \left(\frac{q_{pcomp}}{qpbm} - 1\right) \times 100 \quad (2.50)$$

where, y_{per} and q_{per} denote the error in peak discharge for stage and discharge hydrograph respectively, y_{pcomp} is the computed peak of the stage hydrograph at the outflow section, $ypbm$ is the peak of the benchmark stage hydrograph, q_{pcomp} is the computed peak of the discharge hydrograph at the outflow section, and $ypbm$ is the peak of the benchmark stage hydrograph. The positive values of y_{per} and q_{per} indicate that the peak is overestimated and negative values indicate underestimation of peak values.

2.6.3 Percentage Error in Volume

The percentage error in volume is a measure of conservation of volume during the routing procedure, i.e., how much fraction of volume at the inflow section is being received at the outflow section

$$EVOL = \left(\frac{\sum_{i=1}^{N} Q_{compi}}{\sum_{i=1}^{N} I_i} - 1\right) \times 100 \quad (2.51)$$

Positive value of $EVOL$ indicates a gain of mass and negative value indicates loss of mass. $EVOL$ = 0 indicates that the method satisfies the mass conservation principle.

CHAPTER 3

STUDY AREA

3.1 General

It is considered appropriate to apply the modified VPMS and RCM methods proposed in this study for their field applications over a selected river reach to evaluate the field applicability of the modified methods. Further, it is also necessary to assess the improvements of their performances over the currently available VPMS and RCM methods. To accomplish this proposition, the well gauged 50 km length of the Tiber River in central Italy between Ponte Felcino and Santa Lucia stations, which was used by Silvia et al.(2017) in simulating the observed stage and discharge hydrographs at the Ponte Felcino station using the currently available VPMS method was used.

3.2 The Santa Lucia-Ponte Felcino Section

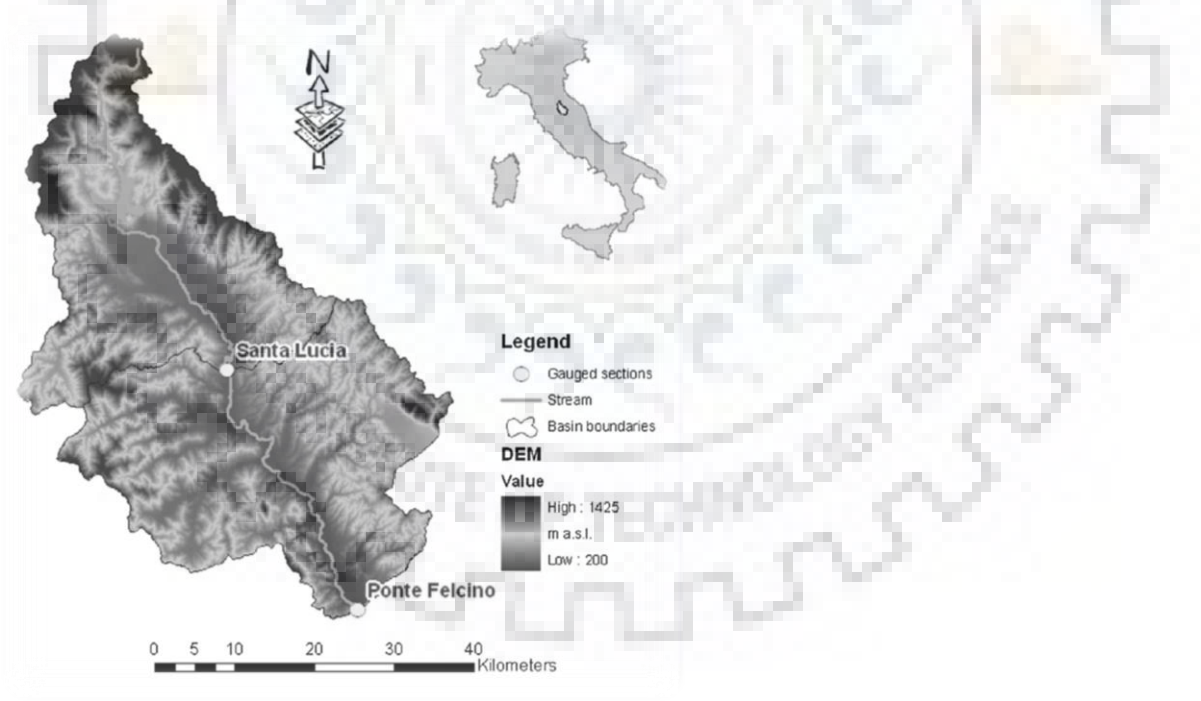

Figure 3-1 Morphology of Tiber River and location of selected river stations(Source: Barbetta et al.(2017))

The Santa Lucia –Ponte Felcino reach data selected for this study has measured cross-sections at 500m intervals and this information has enabled to route hypothetical stage hydrographs using the HEC-RAS model to arrive at the benchmark hydrograph in order to

validate the appropriateness of the modified VPMS method from its theoretical perspectives. The past observed input and reach output stage hydrographs of the floods with significant lateral flow from the intervening catchments are used for the proposed study.

3.3 Determining the Equivalent Channel Section

The VPMS routing technique is applicable for routing in a prismatic channel and, subsequently, its application to a natural river reach requires the assessment of an equivalent prismatic section of the cross-sections at the two ends of the reach which can be obtained by establishing a linear relationship between the actual flow depth and the corresponding prismatic flow depth . The given reach is approximated by an equivalent prismatic section with the help of the information of the cross sections at the ends of the river reaches. As this reach has been extensively studied by Perumal et al.(2010) for the application of the VPMS method for routing, all the conversion equations as developed by Perumal et al.(2017) are directly used in the present study also.

Firstly, the observed stage h is converted to the actual flow depth y_{act} on the basis of the datum level. For the Tiber river, this relationship is expressed as

$$y_{act\_u} = h_u + 0.46 \tag{3.1}$$

$$y_{act\_d} = h_d - 0.36 \tag{3.2}$$

where subscripts u and d refer to the upstream and downstream sections respectively.

Then, the equivalent flow depth and actual flow area relationship is developed along the river reach is expressed as:

$$y_{prism\_u} = 0.833 y_{act\_u} - 0.036 \tag{3.3}$$

$$y_{prism\_d} = 1.149 y_{act\_d} + 0.0421 \tag{3.4}$$

where, y_{prism_u} and y_{prism_d} are the equivalent prismatic depths at the upstream and downstream sections respectively, corresponding to the actual flow depths y_{act_u} and y_{act_d}. For observed flood events, an optimum value of Manning's roughness coefficient n is obtained.

Table 3-1 Selected river reach Lreach=length of reach, Aup and Adown = upstream and downstream flow areas, Aint=intermediate drainage area, S0=mean bed slope, B=mean section width

River	Reach	L_{reach}(km)	A_{up}(km^2)	A_{down}(km^2)	A_{int}(km^2)	S_0	B(m)
Tiber	Santa Lucia-PonteFelcino	50	935	2035	1100	0.0016	35

Table 3-2 Properties of the investigated river reach

Reach	Flood event	Hp_{up}(m)	Qp_{up}(m^{3}s^{-1})	Hp_{down}(m)	Qp_{down}(m^{3}s^{-1})	T_L(h)
Santa Lucia-Ponte Felcino	December1996	4.40	292	4.39	439	4
	November2005	5.61	443	6.92	993	4
	December2005	4.59	314	4.34	430	3
	December2008	4.96	359	4.98	551	4
	November2012	5.62	444	6.03	776	6

CHAPTER 4
METHODOLOGY AND APPROACH

4.1 The prismatic test section

A trapezoidal channel with a bed width of 15 m and side slopes of 1:5 has been used for a distance of 50km. The routing by IVPMS is carried out by dividing the reach into 50 equal sub-reaches ($\Delta x = 1\ km$). No such division of sub-reaches is required for the application of RCM method. The inflow hydrograph adopted is of the form of Pearson type-III distribution and is expressed as

$$\mathrm{I} = I_b + (I_p - I_b)[\frac{t}{t_p}\exp\left(1 - \frac{t}{t_p}\right)]^{\beta} \quad (4.1)$$

where, I_b = 100 m^3s^{-1} ; I_p = 900 m^3s^{-1} , β = 16 ; t_p = 24 h

This inflow hydrograph is used for obtaining the benchmark hydrographs from the HEC-RAS model. For application of the IVPMS and the RCM method, 25 different configurations of the test channel are used. Simulations are done for a routing time interval of 15 minutes.

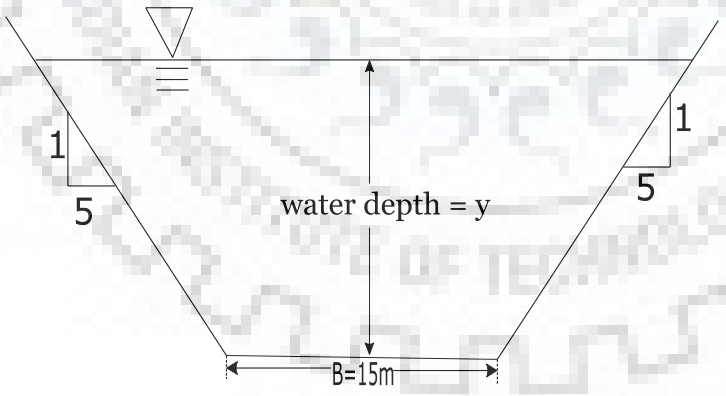

Figure 4-1 Prismatic Trapezoidal Section

Table 4-1 Channel configurations used in the study

Channel Type	Bed Slope	Manning's Roughness
1	0.002	0.01
2	0.002	0.02
3	0.002	0.035
4	0.002	0.04
5	0.002	0.06
6	0.001	0.01
7	0.001	0.02
8	0.001	0.035
9	0.001	0.04
10	0.001	0.06
11	0.0005	0.01
12	0.0005	0.02
13	0.0005	0.035
14	0.0005	0.04
15	0.0005	0.06
16	0.00025	0.01
17	0.00025	0.02
18	0.00025	0.035
19	0.00025	0.04
20	0.00025	0.06
21	0.0001	0.01
22	0.0001	0.02
23	0.0001	0.035
24	0.0001	0.04
25	0.0001	0.06

4.2 The application of VPMS method

As discussed above, the VPMS method follows an iterative procedure to determine the stage as well as discharge at the outflow section. For lateral inflow cases, the lateral flow component q_L has to be computed beforehand in order to incorporate it into the VPMS method. The lateral flow component given by equation (2.36) distributes the lateral flow volume uniformly along the length of the reach. This component gets added to the routing equation of VPMS method to give the stage and discharge at the outflow section. Fig. (4-2) sums up the entire routing procedure of VPMS method:

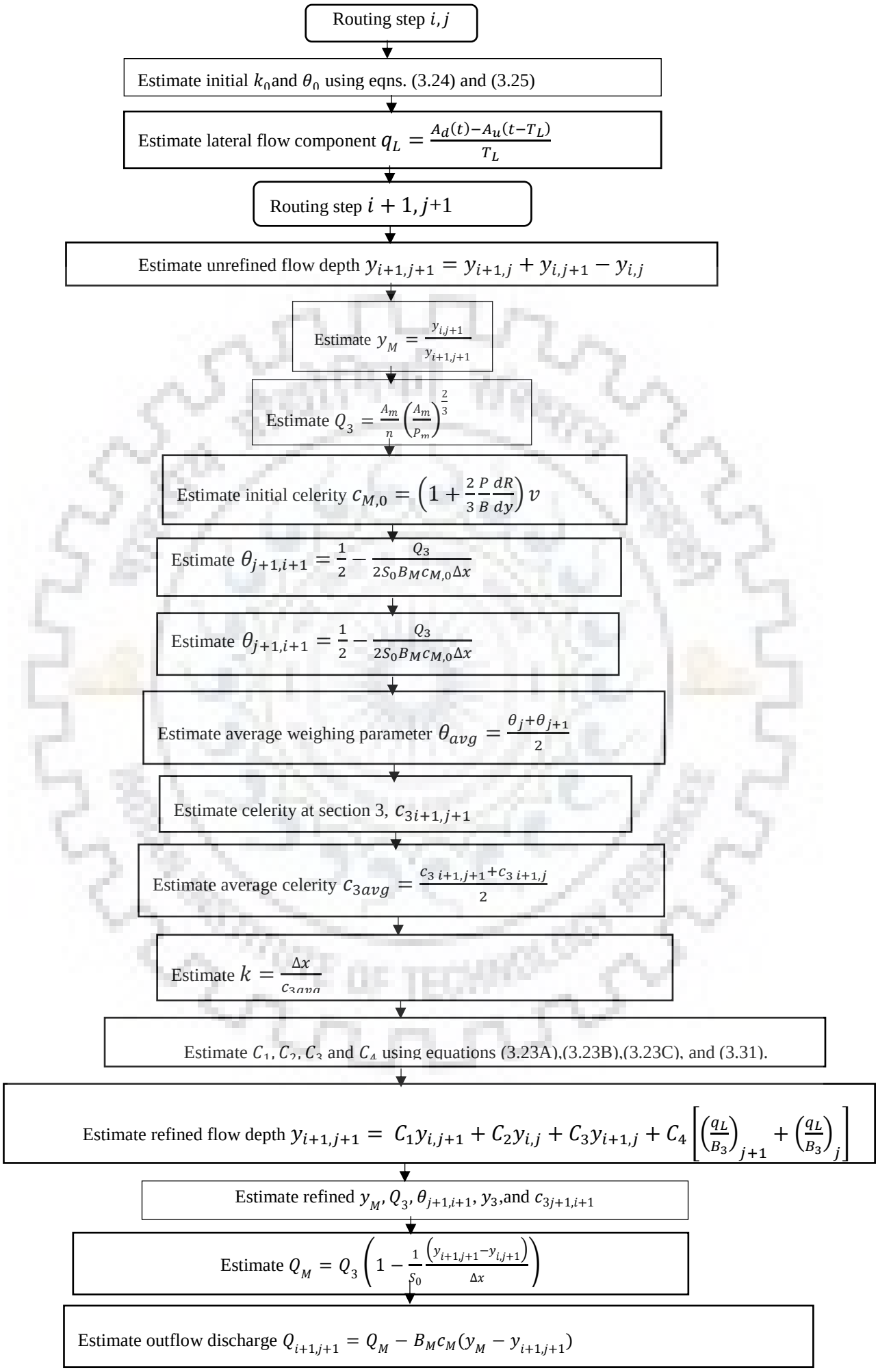

Figure 4-2 Flow chart of VPMS method

4.3 The application of RCM method

From equation (2.37), the governing equation of RCM can be written as

$$Q_D(t) = \alpha \frac{A_D(t)}{A_U(t-T_L)} Q_U(t - T_L) + \beta \quad (4.2)$$

The parameters α and β can be determined by using values of downstream peak discharge $Q_D(T_P)$ and base-flow $Q_D(T_B)$ obtained by equations (2.44) and (2.43) respectively, and the observed flow area and upstream discharge hydrograph. The lateral flow component is computed by the characteristic approach as previously discussed. Figure (4-3) explains the flow transport procedure of the RCM model.

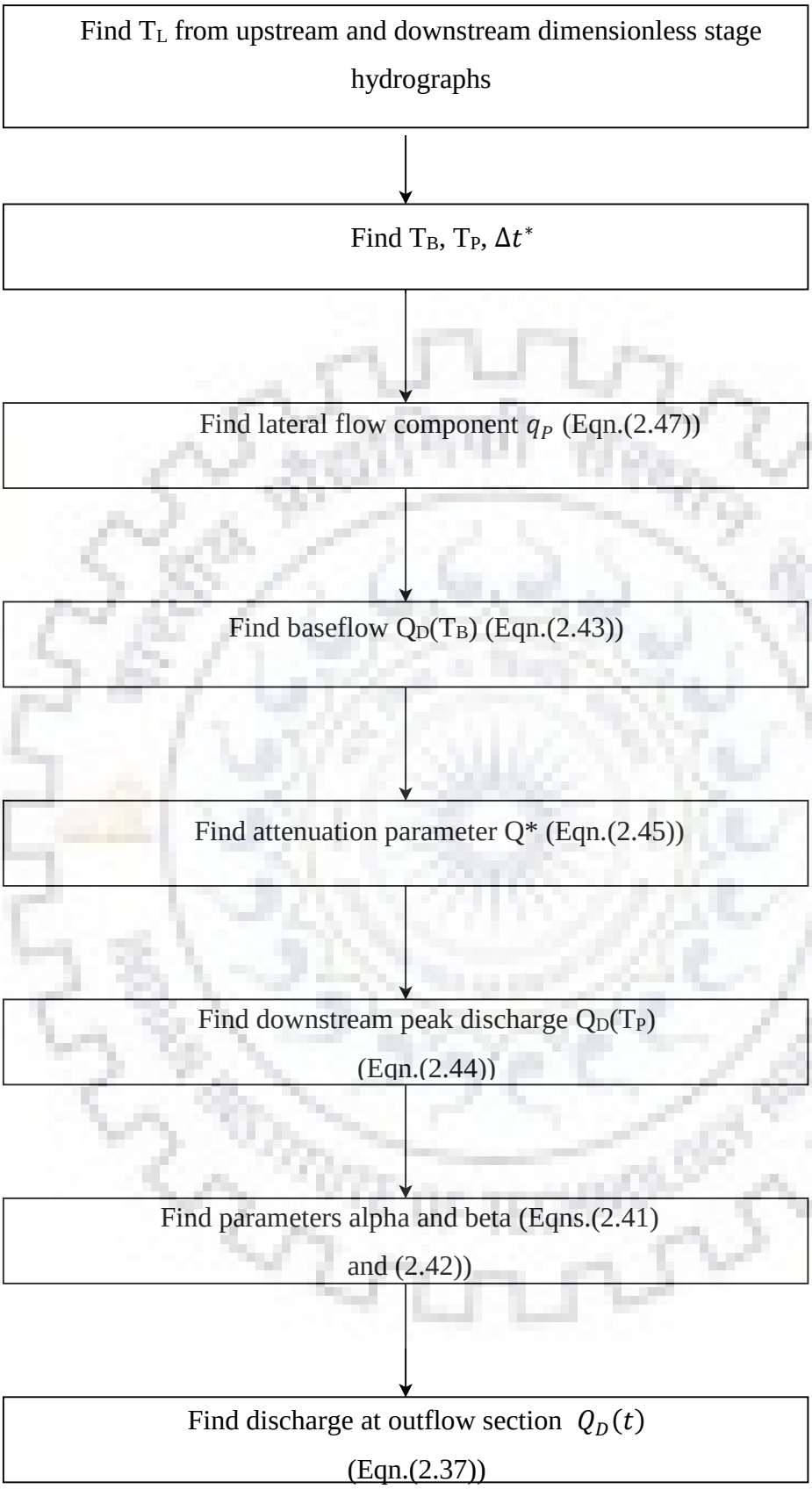

Figure 4-3 Flow Chart of RCM method

4.4 Consideration of constant wave travel time in the VPMS model

In the VPMS method, both the parameters, i.e. wave travel time k and the storage coefficient θ are allowed to vary at every time step. This consideration gains fruition when it comes to unsteady flow conditions where the flow conditions vary with time. But in case of significant lateral inflow conditions, the assumption of variable parameters, especially the wave travel time, may not be accurate. The wave travel time in such a case should be considered constant.

The simple reason behind this consideration is that the incorporation of lateral flow involves the characteristic form of continuity equation, i.e.

$$\frac{dA}{dt} = q_L \tag{4.3}$$

The above equation is valid along a particular characteristic line moving with a certain celerity. But along a characteristic line, the wave moves with the same velocity. If we consider the wave travel time to be varying in the VPMS method with each time step, as is being done in normal scenario, it will not be in accordance with the kinematic nature of the lateral flow component which is getting added along the reach. Thus, we will consider the wave speed or celerity c to be constant in the application of the VPMS method. The value of constant celerity will be given by

$$c = \frac{L_{reach}}{T_L} \tag{4.4}$$

where, L_{reach} is the length of the reach and T_L is the time required to match the rising limb of the upstream and downstream dimensionless stage hydrographs.

It was found that the assumption of constant wave travel time for the entire hydrograph was not enough for accurate reproduction of the benchmark hydrograph. Thus, the wave travel time was varied in certain time ranges keeping it constant over a particular time range. Thus, for different ranges of time interval, we have different lag-time values.

The above methodology has been schematically explained by Fig.4-4. It is clear from the figure three lag-time values have been taken for three different time ranges. For each lag

time value there will be a particular value of celerity associated with it(eqn.(4.4)), and thus different value of parameter K.

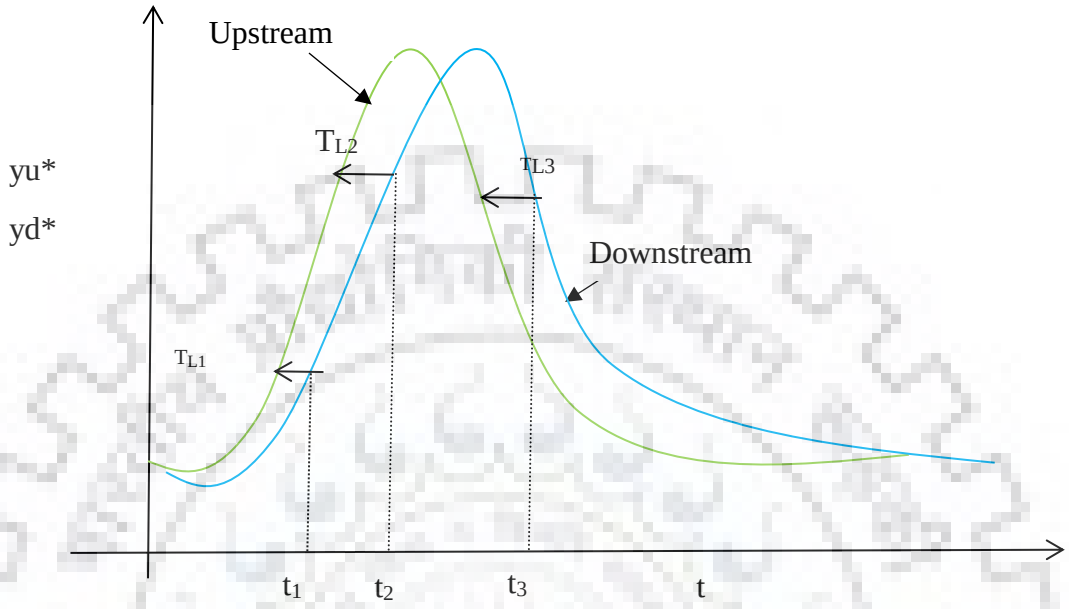

Figure 4-4 Breaking of lag time in different time ranges

4.5 Consideration of variation of lag time in the recession limb of RCM model

The RCM model as proposed by Moramarco et al.(2005) considers the time lag necessary to overlap the rising limb of the upstream and downstream dimensionless hydrographs to be constant for all time steps. This assumption works well for RCM for steeper slopes but for gentle slopes with high roughness values, the model fails to exactly reproduce the benchmark hydrographs. This is reflected in the appearance of deviation in the recession part of the observed hydrograph. In this study, for flatter slopes, the variation of lag time with every time step in the recession part is taken into consideration. A regression fit is obtained between the time ordinates and the lag time. The same relationship is then used in the RCM model for the recession part. The lag time for rising limb, however, is taken as usual.

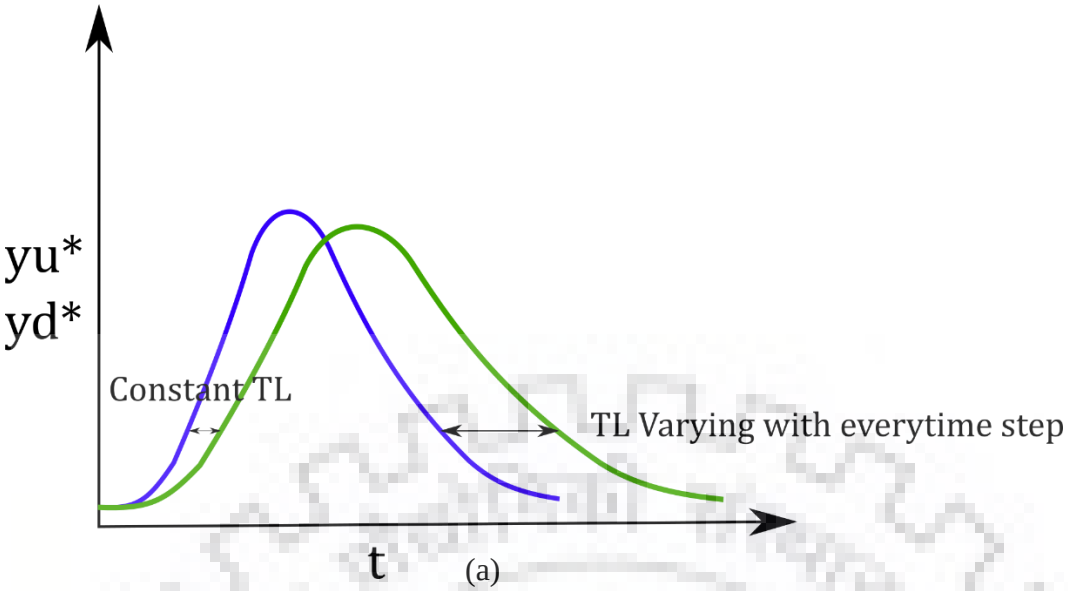

(a)

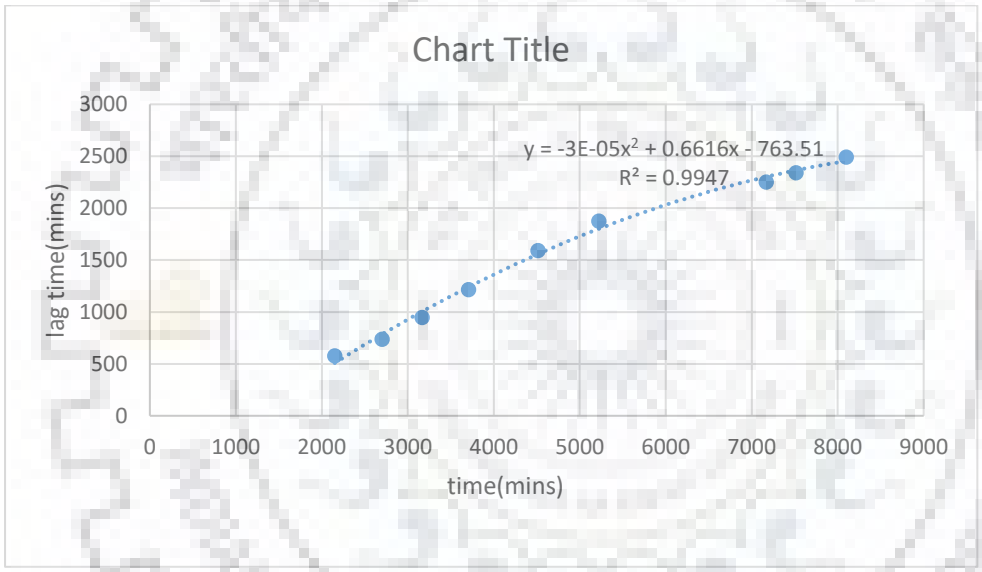

(b)

Figure 4-5 (a) Consideration of lag time in modified RCM, (b) Regression fit between time and lag time for channel type 24

CHAPTER 5
RESULTS AND DISCUSSIONS

Both the methods, i.e., the VPMS(or the improved VPMS method labelled as IVPMS in the figures) and RCM methods are applied on the hypothetical channel section as well as natural river section. The results obtained are compared with the benchmark solutions obtained using HEC-RAS in case of numerical test and with the observed stage and discharge hydrographs in case of field test. The performance of the methods is evaluated on the basis of the various applicability crtiteria defined by Perumal et al.(2007).

5.1 Numerical Test

5.1.1 Discharge reproduction

The VPMS method and the RCM method are first applied to a 50 km long prismatic channel reach having a symmetrical trapezoidal cross-section with bottom width of 15m and with a side slope of 1:5. The inflow hydrograph used to arrive at the benchmark solutions for different channel types considered in the study is defined by the form of Pearson Type-III distribution as given by eqn.(4.1). The routed discharge hydrographs arrived at the outlet of the considered 50 km hypothetical channel reaches of different channel types studied are compared with the corresponding benchmark solutions and the simulation results of the method are evaluated using the performance measured as discuused in section (3.5). The discharge hydrographs obtained at the outlet using the proposed method are compared with respect to the benchmark solutions using the applicability criteria discussed in section (3.5). Routing using the VPMS method was carried out for a spatial interval of 1 km and temporal interval of 15 minutes. For the application of RCM method, there is no need of any spatial interval as it involves a single reach length only, and the time interval used is 15 minutes. Fig.(5-1) shows the reproduction of the benchmark discharge hydrographs by using the VPMS and the RCM methods for all the studied configurations of the trapezoidal channel reach. Table(5-1) shows the performance evaluation criteria for the VPMS and the RCM method compared with the corresponding characteristics of the benchmark solutions obtained using HEC-RAS model. The performance evaluation measures include the Nash-

Sutcliffe Efficiency (η_q in %), the percentage error in peak discharge (q_{per} in %), and the percentage error in volume ($EVOL$ in %).

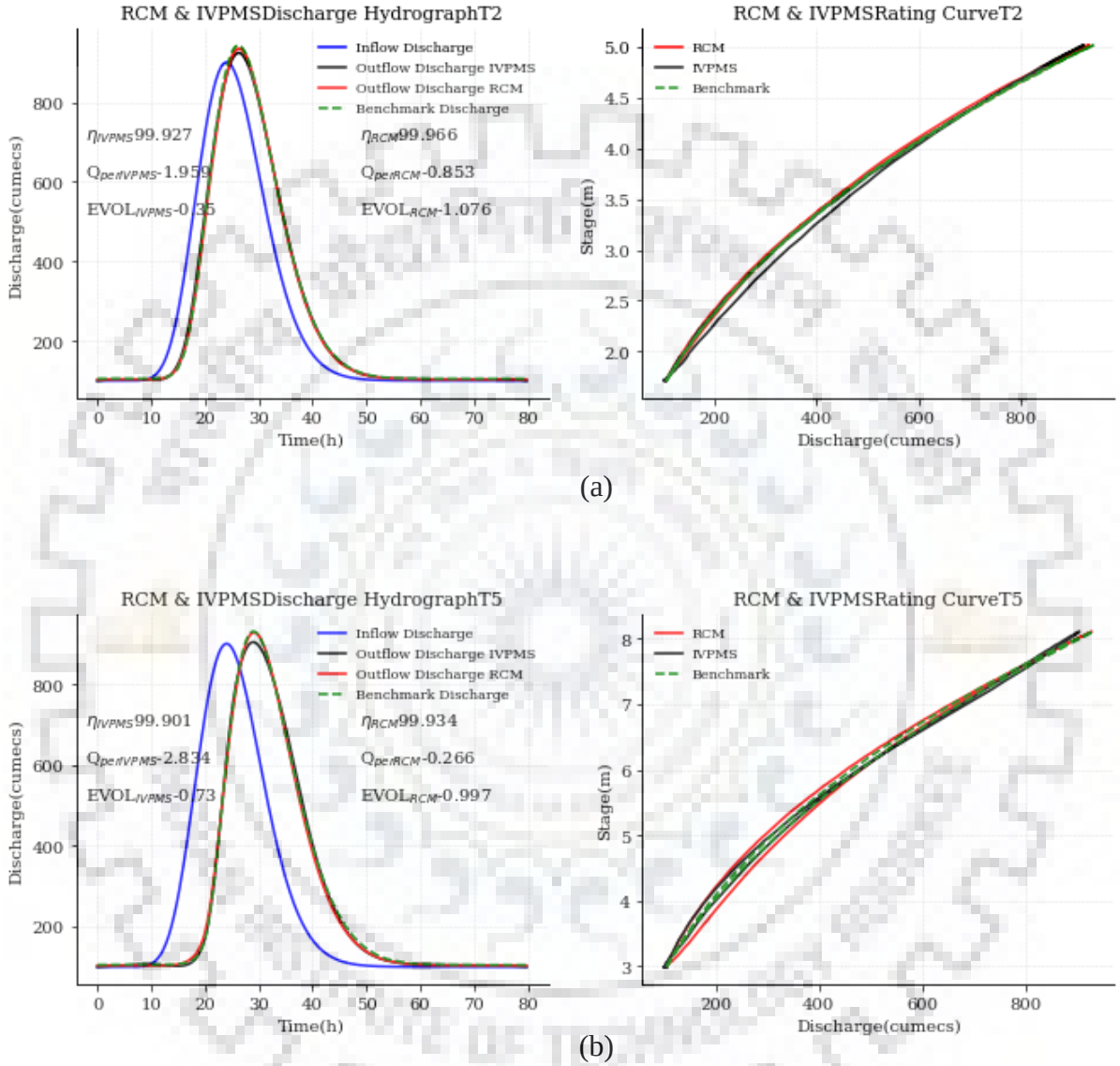

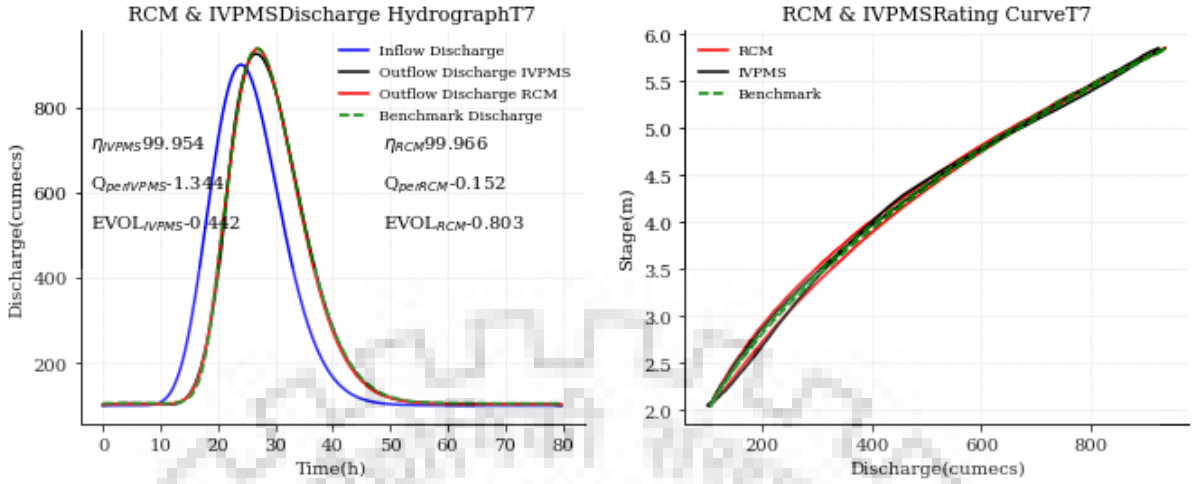
RCM & IVPMSDischarge HydrographT7
Inflow Discharge
Outflow Discharge IVPMS
Outflow Discharge RCM
Benchmark Discharge
ηIVPMS99.954
QpeIVPMS-1.344
EVOLIVPMS-0.442
ηRCM99.966
QpeRCM-0.152
EVOLRCM-0.803
Discharge(cumecs)
Time(h)
RCM & IVPMSRating CurveT7
RCM
IVPMS
Benchmark
Stage(m)
Discharge(cumecs)

(c)

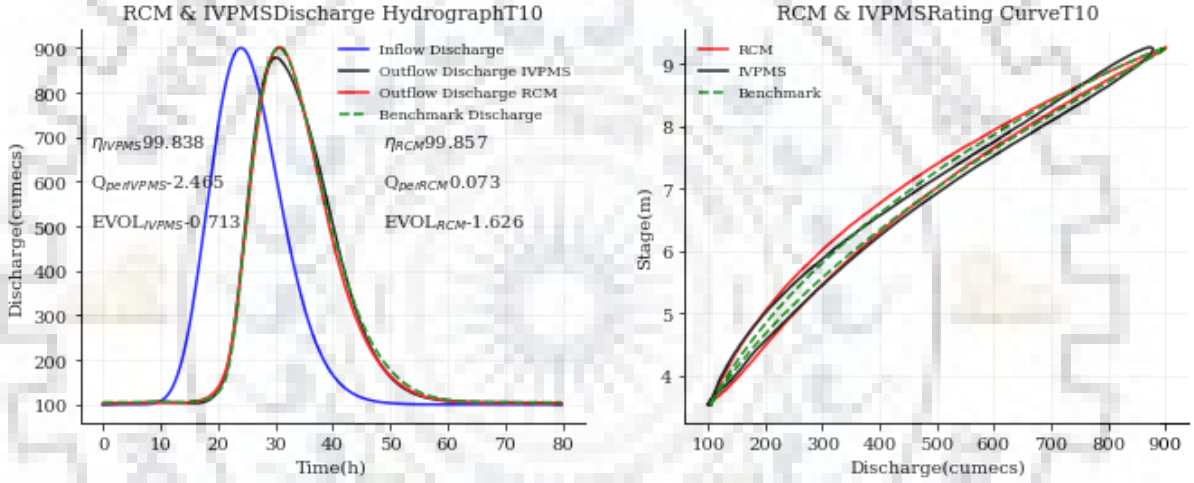
RCM & IVPMSDischarge HydrographT10
Inflow Discharge
Outflow Discharge IVPMS
Outflow Discharge RCM
Benchmark Discharge
ηIVPMS99.838
QpeIVPMS-2.465
EVOLIVPMS-0.713
ηRCM99.857
QpeRCM0.073
EVOLRCM-1.626
Discharge(cumecs)
Time(h)
RCM & IVPMSRating CurveT10
RCM
IVPMS
Benchmark
Stage(m)
Discharge(cumecs)

(d)

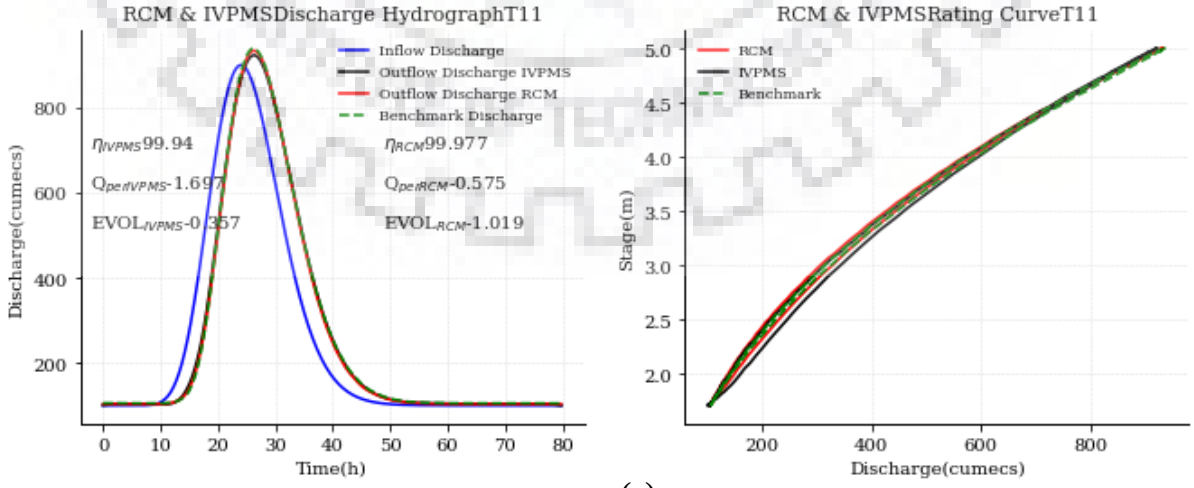
RCM & IVPMSDischarge HydrographT11
Inflow Discharge
Outflow Discharge IVPMS
Outflow Discharge RCM
Benchmark Discharge
ηIVPMS99.94
QpeIVPMS-1.697
EVOLIVPMS-0.357
ηRCM99.977
QpeRCM-0.575
EVOLRCM-1.019
Discharge(cumecs)
Time(h)
RCM & IVPMSRating CurveT11
RCM
IVPMS
Benchmark
Stage(m)
Discharge(cumecs)

(e)

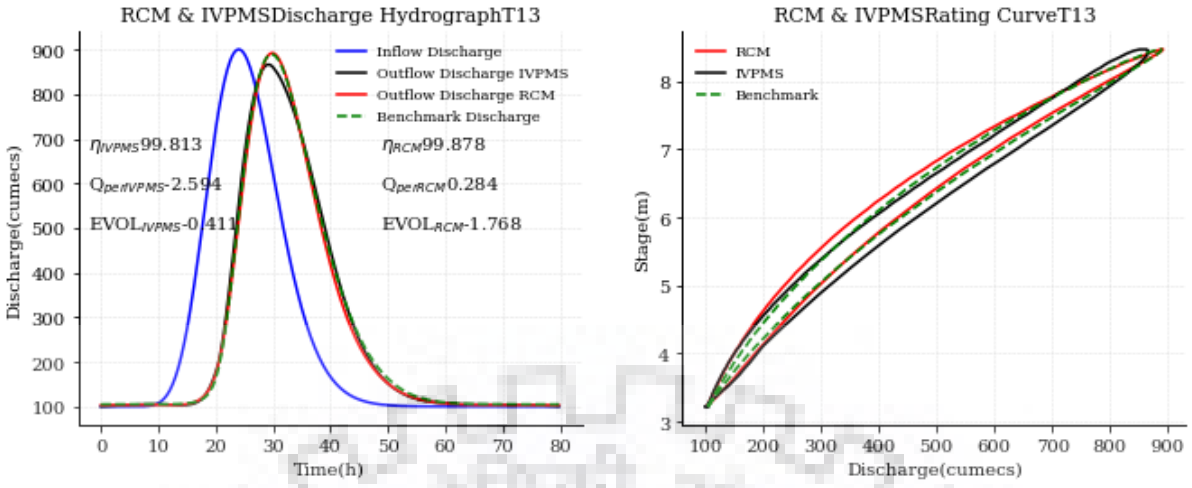
RCM & IVPMSDischarge HydrographT13
Inflow Discharge
Outflow Discharge IVPMS
Outflow Discharge RCM
Benchmark Discharge
ηIVPMS99.813
QperIVPMS-2.594
EVOLIVPMS-0.411
ηRCM99.878
QperRCM0.284
EVOLRCM-1.768
Discharge(cumecs)
Time(h)
RCM & IVPMSRating CurveT13
RCM
IVPMS
Benchmark
Stage(m)
Discharge(cumecs)

(f)

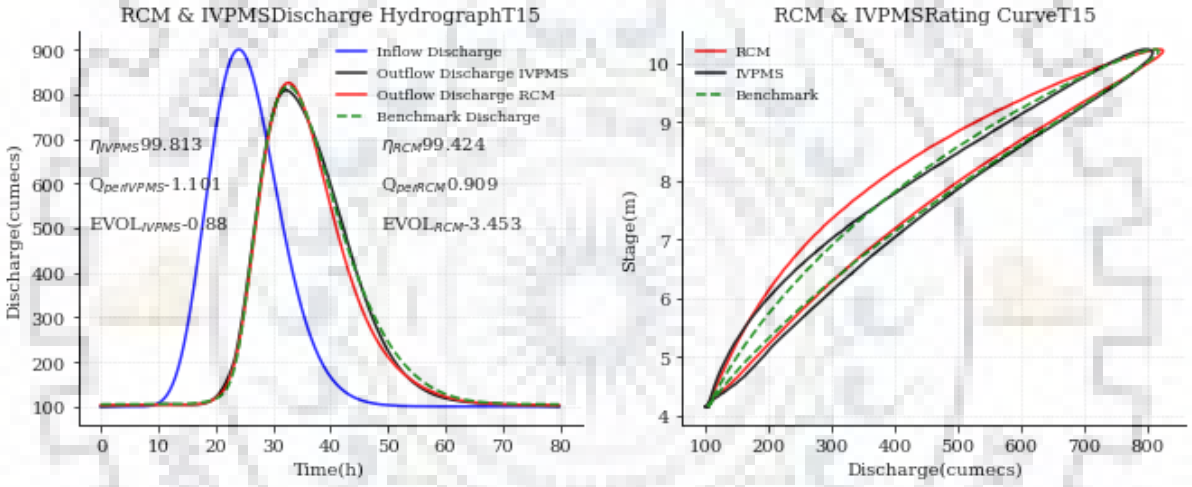
RCM & IVPMSDischarge HydrographT15
Inflow Discharge
Outflow Discharge IVPMS
Outflow Discharge RCM
Benchmark Discharge
ηIVPMS99.813
QperIVPMS-1.101
EVOLIVPMS-0.88
ηRCM99.424
QperRCM0.909
EVOLRCM-3.453
Discharge(cumecs)
Time(h)
RCM & IVPMSRating CurveT15
RCM
IVPMS
Benchmark
Stage(m)
Discharge(cumecs)

(g)

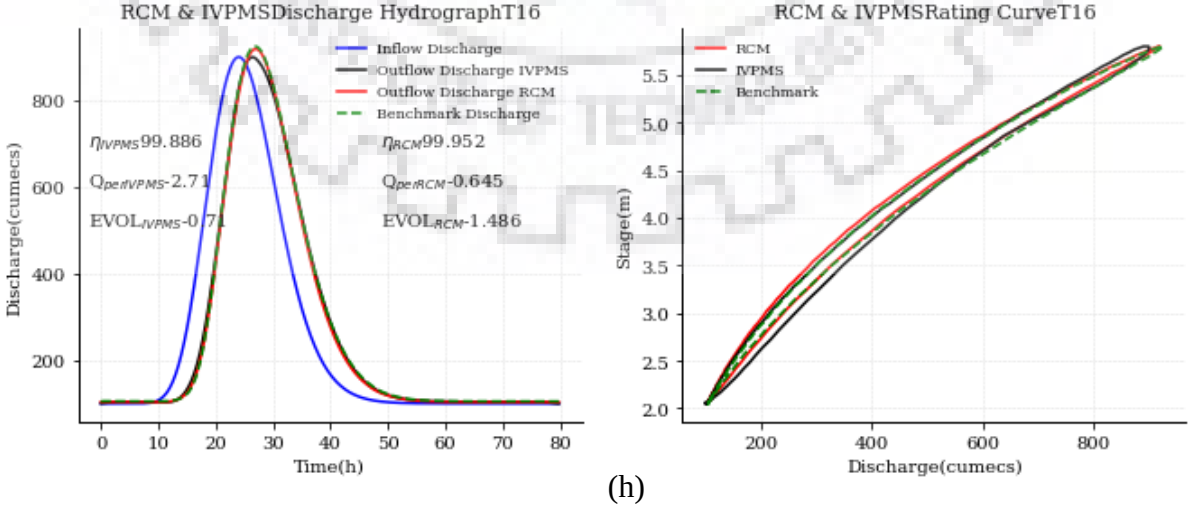
RCM & IVPMSDischarge HydrographT16
Inflow Discharge
Outflow Discharge IVPMS
Outflow Discharge RCM
Benchmark Discharge
ηIVPMS99.886
QperIVPMS-2.71
EVOLIVPMS-0.71
ηRCM99.952
QperRCM-0.645
EVOLRCM-1.486
Discharge(cumecs)
Time(h)
RCM & IVPMSRating CurveT16
RCM
IVPMS
Benchmark
Stage(m)
Discharge(cumecs)

(h)

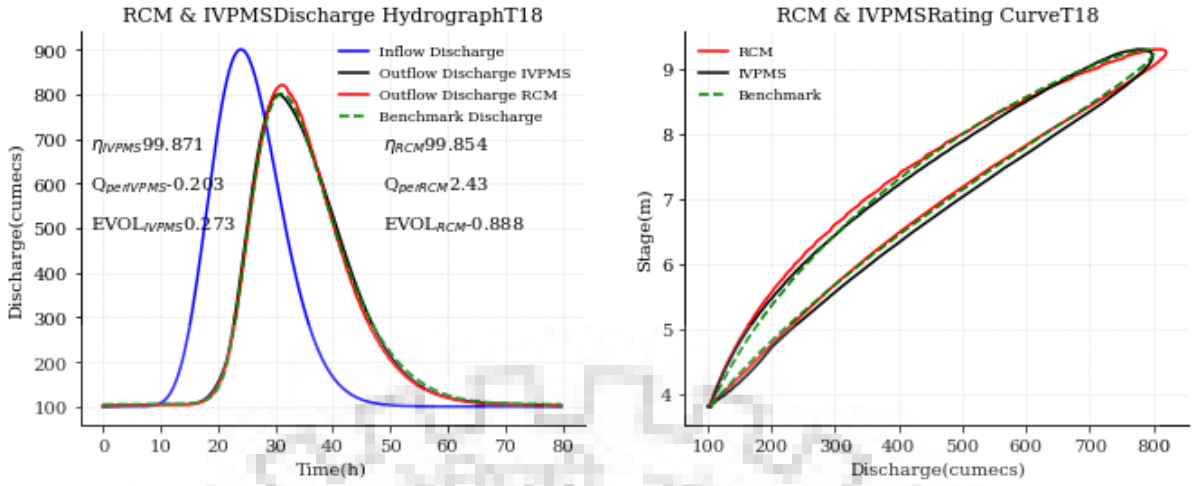
RCM & IVPMSDischarge HydrographT18
Inflow Discharge
Outflow Discharge IVPMS
Outflow Discharge RCM
Benchmark Discharge
ηIVPMS99.871
QpeIVPMS-0.203
EVOLIVPMS0.273
ηRCM99.854
QpeRCM2.43
EVOLRCM-0.888
Discharge(cumecs)
Time(h)
RCM & IVPMSRating CurveT18
RCM
IVPMS
Benchmark
Stage(m)
Discharge(cumecs)

(i)

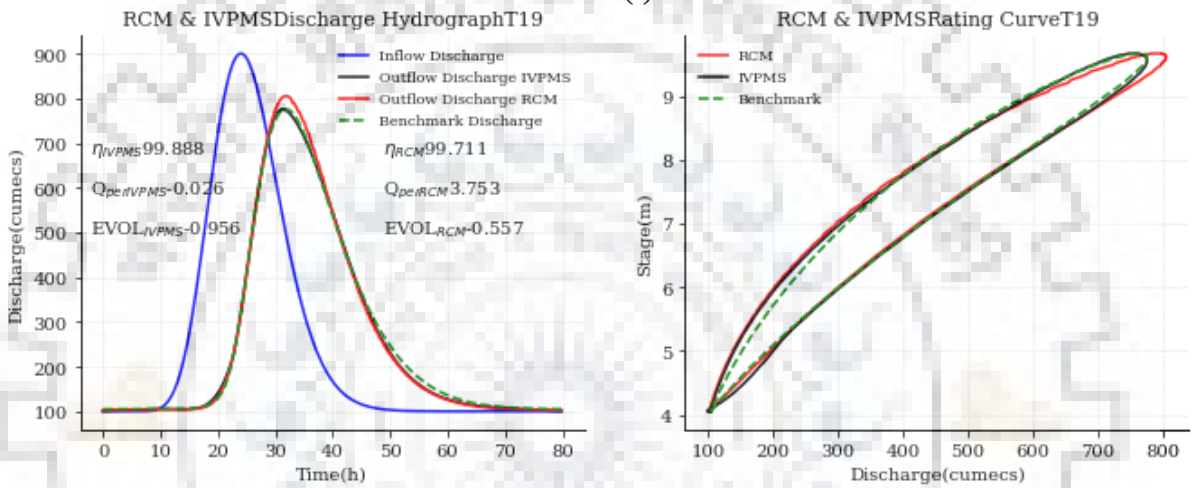
RCM & IVPMSDischarge HydrographT19
Inflow Discharge
Outflow Discharge IVPMS
Outflow Discharge RCM
Benchmark Discharge
ηIVPMS99.888
QpeIVPMS-0.026
EVOLIVPMS-0.956
ηRCM99.711
QpeRCM3.753
EVOLRCM-0.557
Discharge(cumecs)
Time(h)
RCM & IVPMSRating CurveT19
RCM
IVPMS
Benchmark
Stage(m)
Discharge(cumecs)

(j)

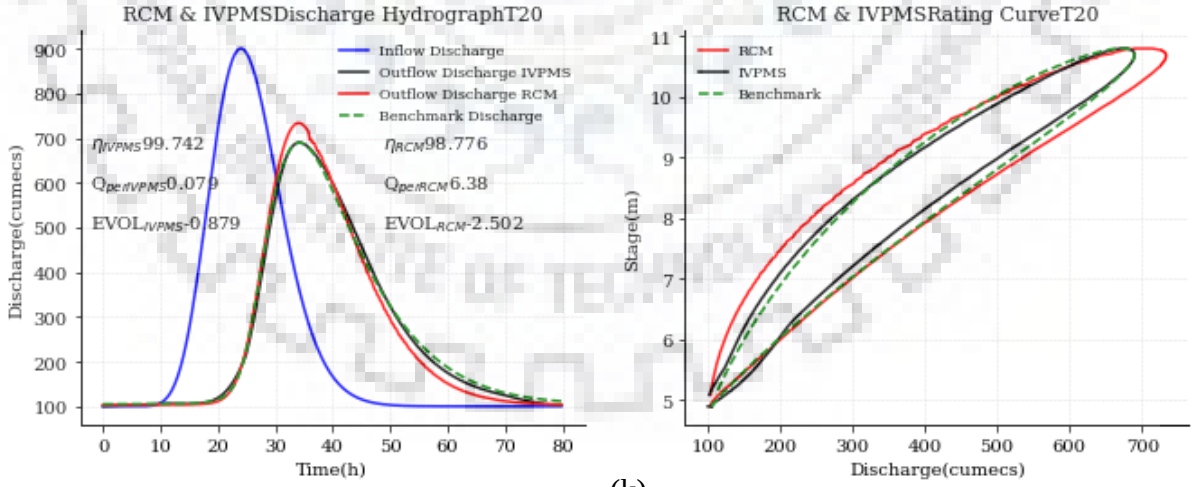
RCM & IVPMSDischarge HydrographT20
Inflow Discharge
Outflow Discharge IVPMS
Outflow Discharge RCM
Benchmark Discharge
ηIVPMS99.742
QpeIVPMS0.079
EVOLIVPMS-0.879
ηRCM98.776
QpeRCM6.38
EVOLRCM-2.502
Discharge(cumecs)
Time(h)
RCM & IVPMSRating CurveT20
RCM
IVPMS
Benchmark
Stage(m)
Discharge(cumecs)

(k)

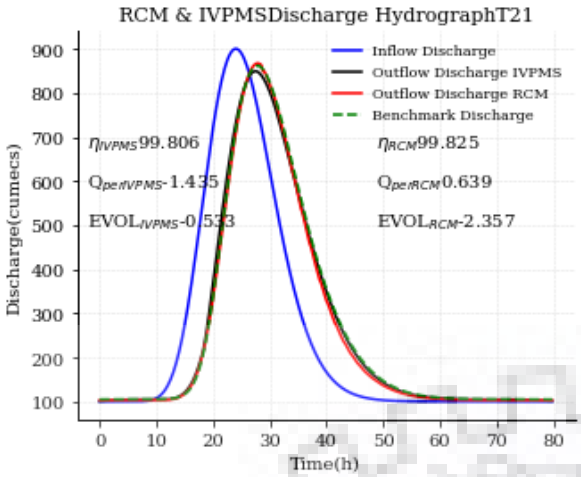
RCM & IVPMSDischarge HydrographT21
Inflow Discharge
Outflow Discharge IVPMS
Outflow Discharge RCM
Benchmark Discharge
ηIVPMS99.806
QpeIVPMS-1.435
EVOLIVPMS-0.533
ηRCM99.825
QpeRCM0.639
EVOLRCM-2.357
Discharge(cumecs)
Time(h)

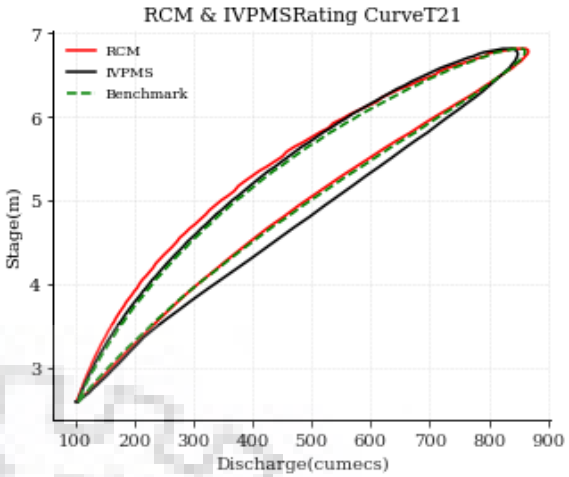
RCM & IVPMSRating CurveT21
RCM
IVPMS
Benchmark
Stage(m)
Discharge(cumecs)

(l)

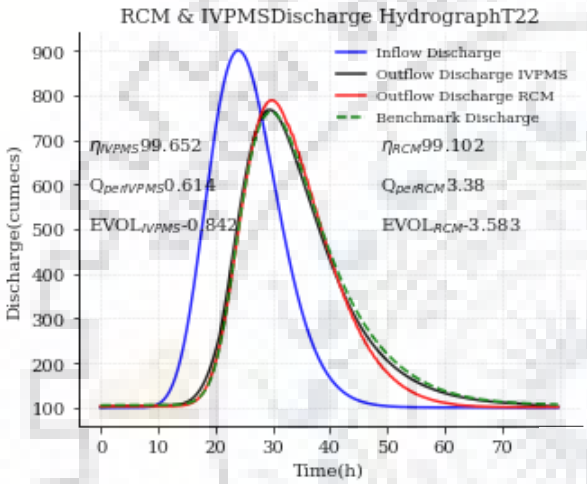
RCM & IVPMSDischarge HydrographT22
Inflow Discharge
Outflow Discharge IVPMS
Outflow Discharge RCM
Benchmark Discharge
ηIVPMS99.652
QpeIVPMS0.614
EVOLIVPMS-0.842
ηRCM99.102
QpeRCM3.38
EVOLRCM-3.583
Discharge(cumecs)
Time(h)

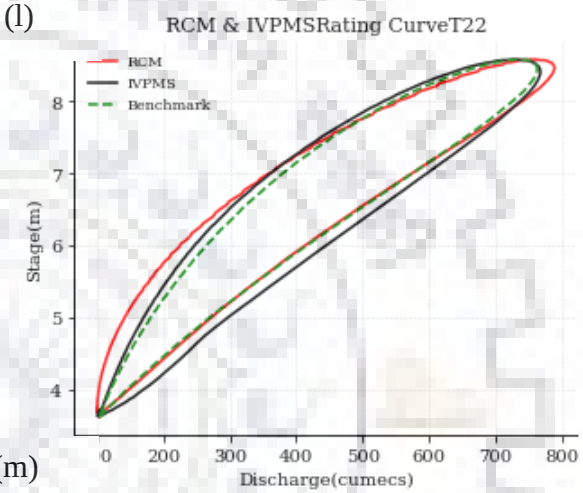
RCM & IVPMSRating CurveT22
RCM
IVPMS
Benchmark
Stage(m)
Discharge(cumecs)

(m)

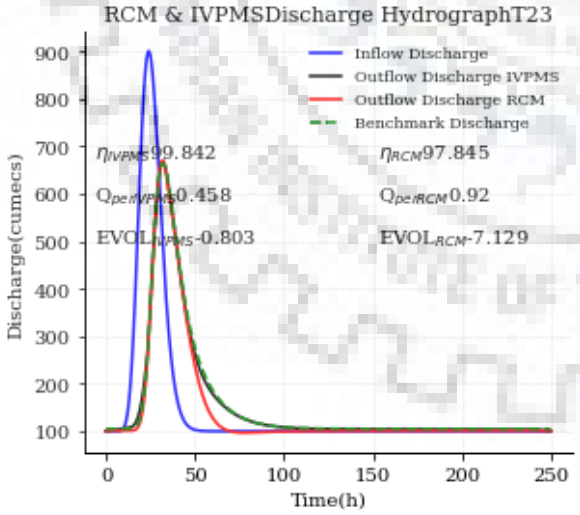
RCM & IVPMSDischarge HydrographT23
Inflow Discharge
Outflow Discharge IVPMS
Outflow Discharge RCM
Benchmark Discharge
ηIVPMS99.842
QpeIVPMS0.458
EVOLIVPMS-0.803
ηRCM97.845
QpeRCM0.92
EVOLRCM-7.129
Discharge(cumecs)
Time(h)

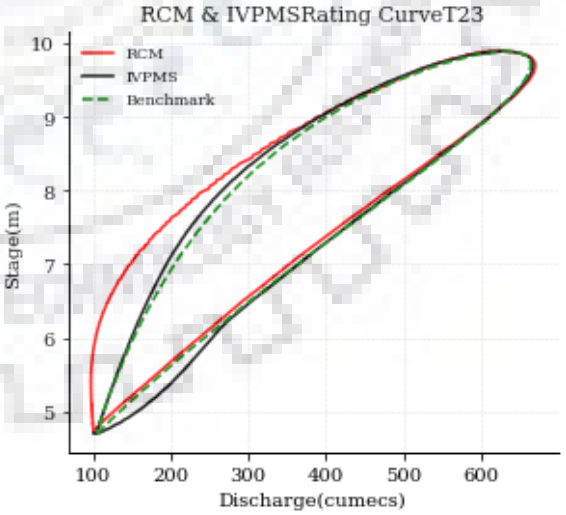
RCM & IVPMSRating CurveT23
RCM
IVPMS
Benchmark
Stage(m)
Discharge(cumecs)

(n)

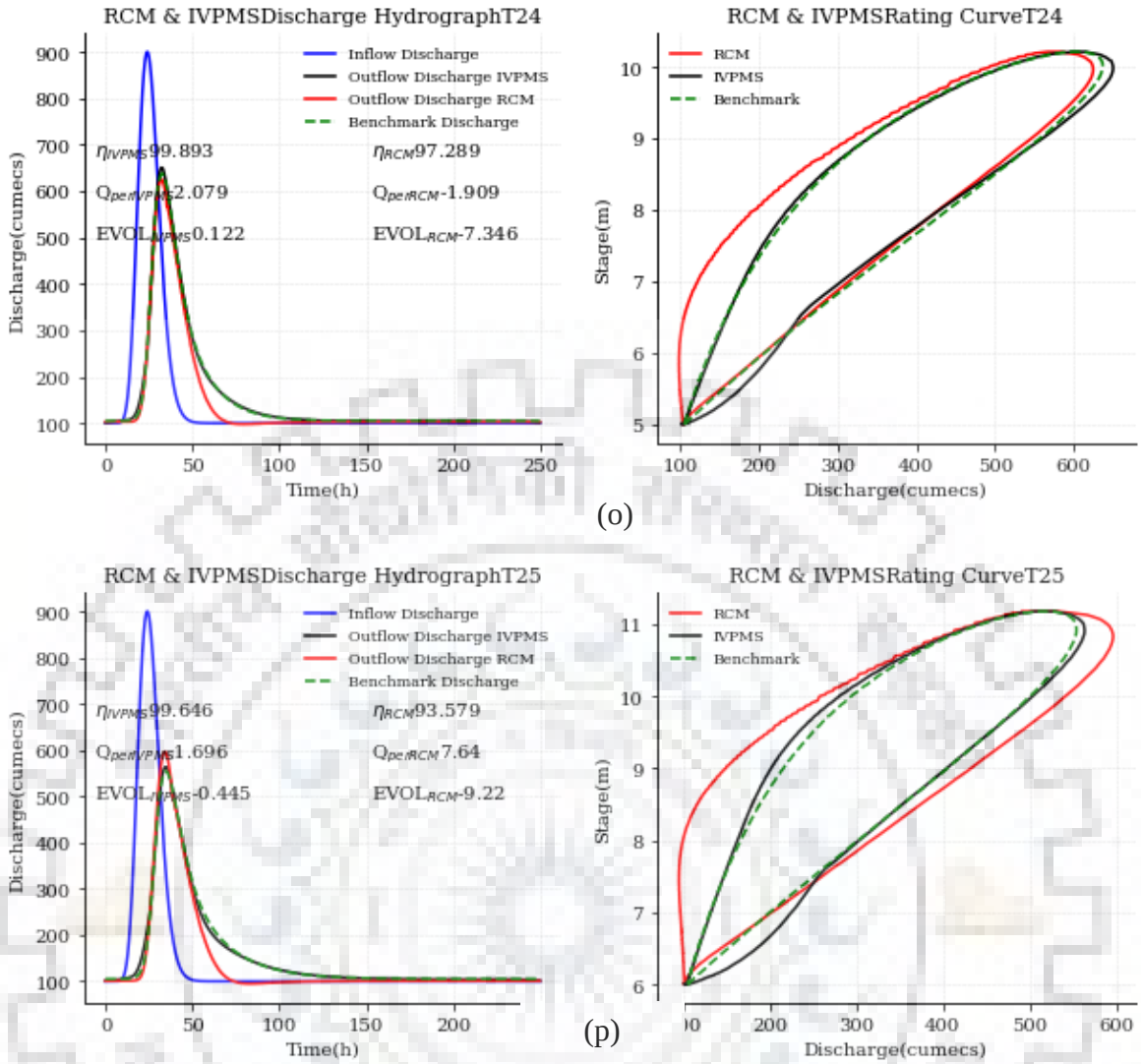

Figure 5-1 Reproduction of benchmark HEC-RAS solutions by the VPMS and RCM methods in test channels(IVPMS stands for the improved or modified VPMS method)

Table 5-1 Summary of performance criteria showing the reproduction of appropriate characteristics of the benchmark HEC-RAS solutions by the VPMS and RCM method applied in trapezoidal channel reaches having reach length of 50 km

	IVPMS					RCM		
Channel Type	η_y **(%)**	y_{per} **(%)**	η_q **(%)**	q_{per} **(%)**	**EVOL(%)**	η_q **(%)**	q_{per} **(%)**	**EVOL(%)**
2	99.925	-0.808	99.927	-1.959	-0.350	99.966	-0.853	-1.076
3	99.907	-0.876	99.908	-2.158	-0.812	99.968	-0.297	-0.851
4	99.845	-1.588	99.753	-3.595	0.061	99.952	-0.694	-1.000
5	99.905	-1.222	99.901	-2.834	-0.730	99.934	-0.266	-0.997
7	99.935	-0.546	99.954	-1.344	-0.442	99.966	-0.152	-0.803
8	99.840	-1.240	99.854	-2.865	-0.256	99.945	-0.261	-1.067
9	99.875	-1.252	99.865	-3.099	-0.525	99.934	-0.145	-1.165
10	99.779	-0.998	99.838	-2.465	-0.713	99.857	0.073	-1.626
11	99.920	-0.626	99.940	-1.697	-0.357	99.977	-0.575	-1.019
12	99.853	-1.911	99.814	-4.364	-1.976	99.877	-0.716	-1.393
13	99.778	-0.940	99.813	-2.594	-0.411	99.878	0.284	-1.768
14	99.804	-0.864	99.857	-2.275	-0.653	99.845	0.612	-1.900
15	99.531	-0.057	99.813	-1.101	-0.880	99.424	0.909	-3.453
16	99.885	-1.070	99.886	-2.710	-0.710	99.952	-0.645	-1.486
17	99.776	-0.879	99.816	-2.395	-0.333	99.831	0.236	-2.231
18	99.654	0.308	99.871	-0.203	0.273	99.854	2.430	-0.888
19	99.600	0.556	99.888	-0.026	-0.956	99.711	3.753	-0.557
20	99.280	1.439	99.742	0.079	-0.879	98.776	6.380	-2.502
21	99.769	-0.347	99.806	-1.435	-0.533	99.825	0.639	-2.357
22	99.463	0.361	99.652	0.614	-0.842	99.102	3.380	-3.583
23	99.193	1.041	99.646	1.146	-1.366	97.845	0.92	-7.129
24	98.664	1.881	99.583	2.766	-0.772	97.289	-1.909	-7.346
25	96.972	2.872	98.806	2.183	-1.206	93.579	7.64	-9.22

It can be inferred from Fig.5-1 and from the summary of reproduction results given in Table 5-1 in reproducing some pertinent characteristics of the hypothetical benchmark solutions, that both the VPMS and RCM methods are able to reproduce the benchmark solutions closely, with overall close reproduction of the entire benchmark solutions being achieved by the modified VPMS method in comparison with that of the RCM method. But considering the performance measure of q_{per}(%), measuring the error between the benchmark and that simulated by the VPMS and the RCM methods, the RCM method scores better than the proposed modified VPMS method in closely reproducing the peak discharge of the benchmark solution. However, this remark on close reproduction by the RCM method does not imply that the VPMS method poorly reproduces the peak discharge estimate of the benchmark solution, as the performance comparison is only a relative statement and the VPMS method's estimated peak discharge is still within the acceptable error limit of 5%. However, the other performance measure related to volume error in reproducing both the inflow hydrograph and the lateral flow volume, the VPMS method results reveal that this method is more volume conservative than the RCM method. Though the successful application of the VPMS method requires the fulfillment of the criterion that $\frac{1}{S_0}\frac{\partial y}{\partial x} \leq 0.5$(Perumal and Sahoo,2007), the method is able to reproduce the benchmark solutions closely even when the maximum estimate of $\frac{1}{S_0}\frac{\partial y}{\partial x} \approx 0.75$, as in the case of channel type 25, which is characterized by a very small slope of 0.0001 and Manning's roughness coefficient of 0.06.

From Fig. 5-1, it can also be seen that the performance of the RCM in reproducing the benchmark solutions is comparatively better than that of the VPMS method in cases of channel type 2 to 17. However, from channel type 18 onwards, the recession part of the outflow discharge hydrograph by the RCM method tends to arrive earlier than the corresponding part of the benchmark hydrograph. This is reflected from the slightly lower NSE values obtained by the RCM value as compared to the VPMS method for channel type 18 to 25. Thus, for steeper slopes, the RCM method fares slightly better as compared to the VPMS method, but for flatter slopes the VPMS method performs better than the RCM method.

Considering the performance of both VPMS and RCM methods with $\eta_q \approx 99\%$ or more as being near in reproducing the benchmark solution, it can very well may be seen from Fig.5-1 that such a nearby propagation is conceivable when the slopes are relatively steep, characterized by scaled water surface gradient $\frac{1}{S_0}\frac{\partial y}{\partial x} \leq 0.5$. Under this condition, it appears that there is no noteworthy contrast in the exhibitions of the VPMS and RCM techniques in recreating the benchmark solutions.

Overall, it can also be seen from Table 5-1 that for all the channel configurations, the percentage error in peak is less than the acceptable value of $|y_{per}| < 5\%$ for both the methods. Also, the percentage error in volume is less than the acceptable value of $|EVOL| < 5\%$.

5.2 Comparison of the results of the VPMS method with and without modification of the wave travel time

As already discussed, the VPMS method used in this study involves the use of constant wave travel time K unlike its original form which considers the wave travel time to be varying in each time step.

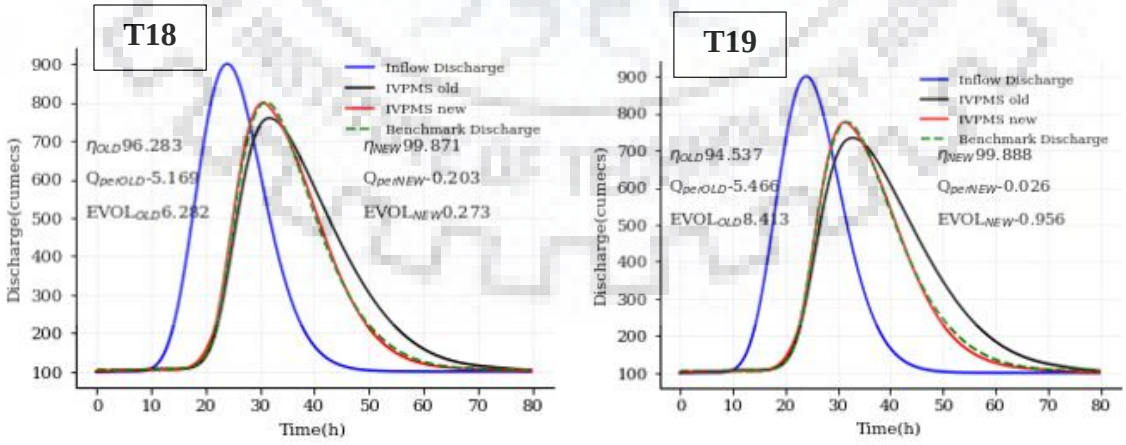

\

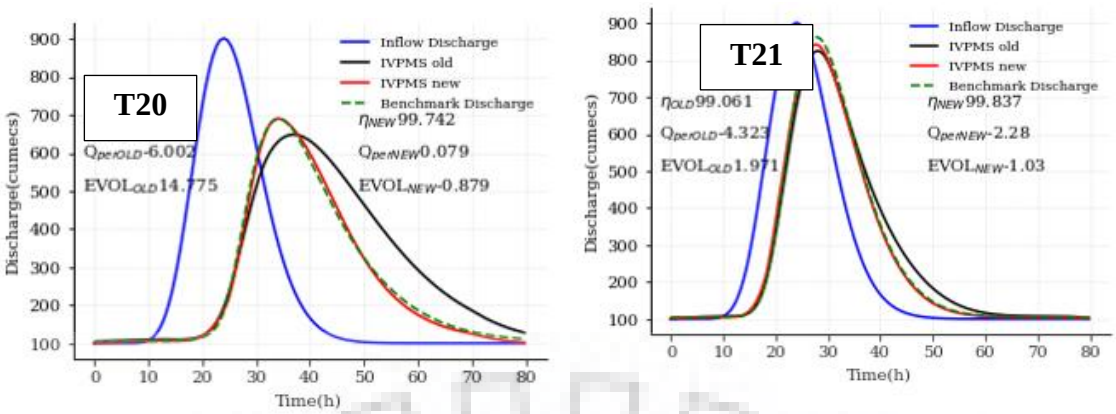

Figure 5-2 Comparison of original and modified VPMS method(old method stands for the VPMS method in its earlier form, i.e. having all parameters variable, new method stands for the modified VPMS method being discussed in the text)

Figure 5-2 represents the reproduction of the benchmark hydrographs by the VPMS method considering constant wave travel time in one case(labelled as new method in Fig.5-2) and variable wave travel time in another(labelled as new method in Fig.5-2), for channel type 18 to 21. It is evident from the figure that the performance evaluation criteria for the modified VPMS method fares much better than that for the earlier method as studied by Silvia et al.(2017)(shown as IVPMS old in Fig.5-2). This justifies our assumption of constant wave travel time in the case of significant lateral inflow conditions.

5.3 Comparison of the results of the RCM method with and without modification of the wave travel time

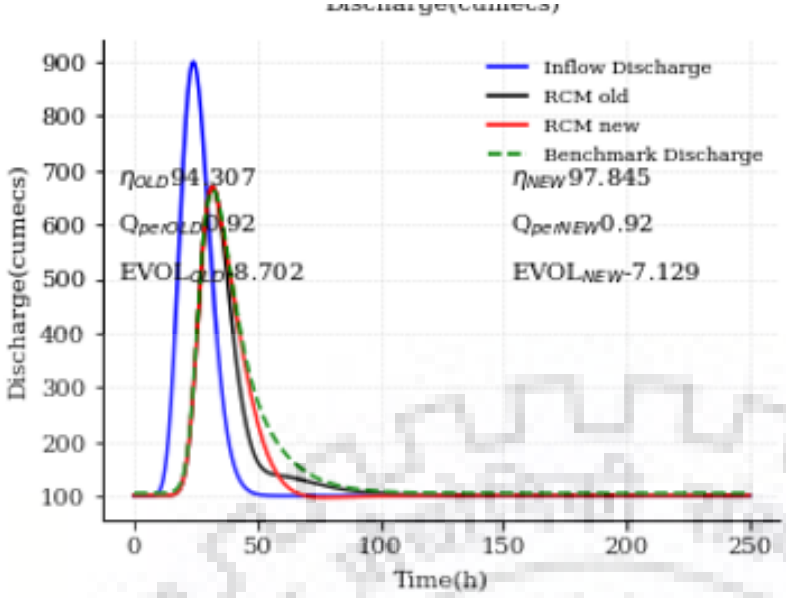

Figure 5-3Comparision of results obtained by RCM method with and without modification of wave travel time for channel type 25

The wave travel time used in the RCM in its original formulation(Moramarco et al.,2005) is constant throughout the entire time interval. However, in this study, the wave travel time has been modified such that in the rising portion of the hydrograph, it remains constant but in the recession part, it varies with time interval. Thus, a regression fit is obtained between the lag-time and the time ordinates. This regression equation is used to obtain the lag-time required at every time step in the recession part of the hydrograph. As it is evident from figure 11, the benchmark hydrograph is better reproduced in the recession part by the hydrograph obtained using this modification as compared to the hydrograph obtained by using the original RCM.

5.4 Field Data Results

he RCM and the VPMS are applied to the 50 km long reach of the Tiber River in central Italy between Santa Lucia gauging site, which is the inlet section of the reach and Ponte Felcino, which is the outlet section of the reach. The hydraulic characteristics of the reach are already being discussed in section 4.2.

Both the methods are checked for their application for different selected flood events. The optimal value of the Manning's roughness coefficient(n_{opt}) is determined by maximising the value of NSE, which corresponds to the minimum value of RMSE.

Table 5-2 Summary of the performance evaluation criteria of the VPMS and RCM methods for the selected flood events on Tiber River

	STAGE VPMS		**DISCHARGE VPMS**		**DISCHARGE RCM**	
Flood event	η_y **(%)**	y_{per} **(%)**	η_q **(%)**	q_{per} **(%)**	η_q **(%)**	q_{per} **(%)**
Nov-05	98.188	7.841	94.128	12.087	97.291	-4.854
Dec-05	99.039	0.259	94.001	21.168	92.682	-5.370
Dec-08	97.315	4.044	94.666	15.435	92.397	-8.562
Nov-12	95.371	1.499	94.513	6.859	73.018	20.756

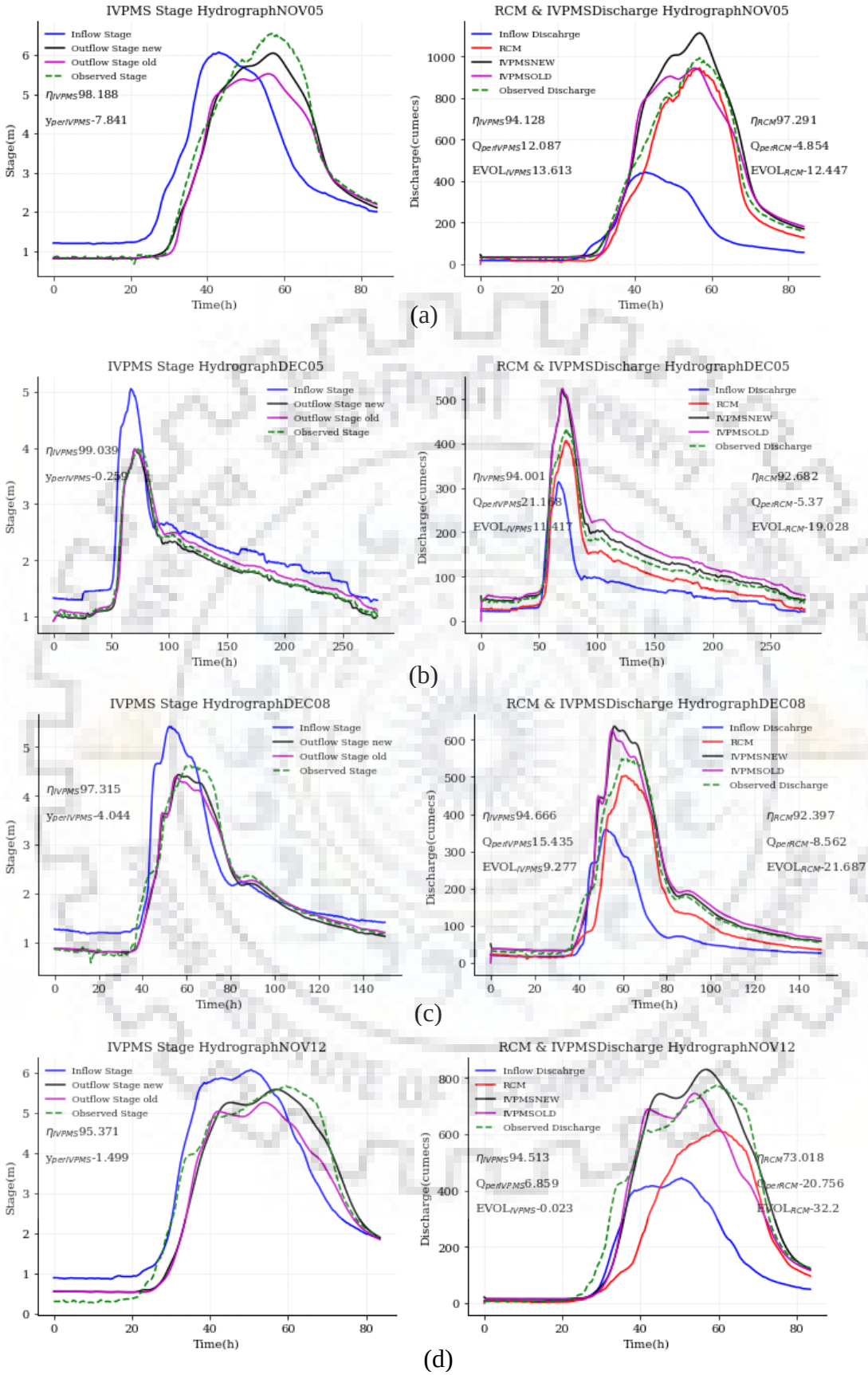

Figure 5-4 Comparison between observed and simulated flow depths and discharges at Ponte Felcino section for the flood occured on a) November 2005b) December 2005 c) December 2008 d) November 2012

Figure 5-4 shows the results obtained at the Ponte-Felcino section of the Santa Lucia-Ponte Felcino section of the Tiber river for four different flood events. Figure 5-1 clearly demonstrates that both the VPMS and the RCM methods are able to reproduce the observed stage and discharge hydrographs fairly accurately. This is being reflected with a higher estimate of NSE(%).

Also, the results obtained by the application of VPMS method considering constant wave travel time are better as compared to when it is applied by taking all the parameters as variable, as is evident from the higher NSE values .

Table 5-3 Comparision of the results obtained by the VPMS method with and without modification

	STAGE				**DISCHARGE**			
Flood event	η_{yold} (%)	η_{ynew} (%)	y_{perold} (%)	y_{pernew} (%)	η_{qold} (%)	η_{qnew} (%)	q_{perold} (%)	q_{pernew} (%)
Nov-05	94.53	98.19	-15.91	-7.84	95.53	94.13	-4.99	12.09
Dec-05	97.93	99.04	0.06	-0.26	85.78	94.00	21.78	21.17
Dec-08	96.34	97.31	-4.91	-4.04	94.43	94.67	13.71	15.43
Nov-12	91.73	95.37	-7.24	-1.50	89.90	94.51	-4.03	6.86

CHAPTER 6
CONCLUSION

In this study, an attempt is made to determine the discharge hydrograph at the downstream section of a considered river reach receiving considerable lateral flow along its length, using the VPMS and RCM methods. The results at the downstream section of the considered channel or river reach are obtained by the former method using method of characteristics to estimate the lateral flow of the sub-reach or reach, followed by the routing approach as built-in in the VPMS method. However, the RCM method straight away adopts the method of characteristics to arrive at the discharge hydrograph at the downstream of the reach. Both the models are checked for their numerical applicability by carrying a number of numerical experiments based simulations. Also, their application to field problem is also demonstrated. Both the methods are compared for their performance in different types of hypothetical channel reaches. Based on the results obtained by the numerical tests, a point by point comparison can be made between the two methods:

1. Both the RCM and the VPMS models are able to simulate the observed/benchmark hydrographs accurately for steeper slopes or slopes characterized by the condition $\frac{1}{S_0}\frac{\partial y}{\partial x} \leq 0.2$ at the inlet of the considered reach corresponding to the hydrograph to be routed. However, the RCM method gives slightly better results than the VPMS method for steep slope channels.

2. For flatter slope channel with high roughness coefficients, the RCM model tends to vary from the observed hydrograph only in the recession part. This variation is attributed to the dynamic nature of flood wave in the recession part of the hydrograph. This problem is being addressed by taking into account the variation of wave travel time with time, but still some variation persists.

3. For the VPMS model used with variable parameters also, the problem of inaccurate reproduction of recession limb occurs. Thus, the parameter k , which represents the wave travel time to be constant along the reach. In this case, we are able to obtain quite a fair reproduction of the recession part of the observed hydrograph.

4. In RCM model, the only information required is the upstream and downstream flow area and the upstream discharge hydrograph. It does not require any information about the cross-section details of the channel. The VPMS method, on the other hand, involves the use of an equivalent prismatic channel section, which is obtained by the topographical information about the channel section.

Thus, we have seen that both the methods are suitable for studying flood wave movements in a channel reach with presence of lateral flow. Both the methods are useful for developing normal stage-discharge relationships for sites where discharge measurement is difficult, or where only the stage is monitored. Moreover, since only stage measurement is involved, the methods prove to be quite advantageous from economic and safety consideration.

REFERENCES

Apollov, B. A., G. P. Kalinin, and V. D. Komarov (1964), Hydrological Forecasting, translated from Russian, Isr. Program for Sci. Transl., Jerusalem

Barbetta, S., Moramarco, T., & Perumal, M. (2017). A Muskingum-based methodology for river discharge estimation and rating curve development under significant lateral inflow conditions. *Journal of Hydrology*, *554*, 216–232. https://doi.org/10.1016/j.jhydrol.2017.09.022

Chow, V. T. (1959). Open channel hydraulics. McGraw-Hili Book Co. Inc., New York, N.Y.

Chiu, C. L., and Tung, N. C. (2002). "Maximum velocity and regularities in open-channel flow." J. Hydraul. Eng., 128(4), 390–398.

Henderson, F. M. (1966). Open channel flow. Macmillan and Co., New York, N.Y.

Moramarco, T., & Singh, V. P. (2000). A practical method for analysis of river waves and for kinematic wave routing in natural channel networks. *Hydrological Processes*, *14*(1), 51–62. https://doi.org/10.1002/(SICI)1099-1085(200001)14:1<51::AID-HYP909>3.0.CO;2-Z

Moramarco, Tommaso, Barbetta, S., Melone, F., & Singh, V. P. (2005). Lateral Inflow, *10*(May 2012), 58–69. https://doi.org/10.1061/(ASCE)1084-0699(2005)10

Moramarco, Tommaso, & Singh, V. P. (2001). S IMPLE METHOD FOR R ELATING LOCAL STAGE AND REMOTE DISCHARGE, *6*(February), 78–81.

Moramarco, T., Saltalippi, C., and Singh, V. P. (2004). "Estimation of mean velocity in natural channels based on Chiu's velocity distribu- tion equation." J. Hydrologic Eng.,9(1), 42–50.

O'donnell, T. (1985). A direct three-parameter muskingum procedure incorporating lateral inflow. *Hydrological Sciences Journal*, *30*(4), 479–496. https://doi.org/10.1080/02626668509491013

Perumal, M. (1994). Hydrodynamic derivation of a variable parameter muskingum method: 1. Theory and solution procedure. *Hydrological Sciences Journal*, *39*(5), 431–442. https://doi.org/10.1080/02626669409492766

Perumal, M., Moramarco, T., Sahoo, B., & Barbetta, S. (2007). A methodology for discharge estimation and rating curve development at ungauged river sites. *Water Resources Research*, *43*(2), 1–22. https://doi.org/10.1029/2005WR004609

Perumal, M., & Price, R. K. (2013). A fully mass conservative variable parameter McCarthy – Muskingum method : Theory and verification. *Journal of Hydrology*, *502*, 89–102. https://doi.org/10.1016/j.jhydrol.2013.08.023

Perumal, M., & Sahoo, B. (2007). Applicability criteria of the variable parameter Muskingum stage and discharge routing methods, *43*(May), 1–20. https://doi.org/10.1029/2006WR004909

Perumal, M., Moramarco, T., Sahoo, B., Barbetta, S., 2010. On the practical applicability of the VPMS routing method for rating curve development at ungauged river sites. Water Resour. Res. 46, W03522. http://dx.doi.org/ 10.1029/2009WR008103

Price, R. K. (1974). Flood routing methods for British rivers.

Swain, R., & Sahoo, B. (2015). Variable parameter McCarthy–Muskingum flow transport model for compound channels accounting for distributed non-uniform lateral flow. *Journal of Hydrology*, *530*, 698–715. https://doi.org/https://doi.org/10.1016/j.jhydrol.2015.10.030

Tarpanelli, A., Barbetta, S., Brocca, L., & Moramarco, T. (2013). River discharge estimation by using altimetry data and simplified flood routing modeling. *Remote Sensing*, *5*(9), 4145–4162. https://doi.org/10.3390/rs5094145

Xia, R. (1997). "Relation between mean and maximum velocities in a natural river." J. Hydraul. Eng., 123(8), 720–723.

Yadav, B., Perumal, M., Bardossy, A., 2015. Variable parameter McCarthy– Muskingum routing method considering lateral flow. J. Hydrol. 523, 489–499. http://dx.doi.org/10.1016/j.jhydrol.2015.01.068

Appendix A

Python code for VPMS

```
# -*- coding: utf-8 -*-
"""
Created on Thu Apr 25 10:26:52 2019

@author: NISHANT
"""

# -*- coding: utf-8 -*-
"""
Created on Fri Mar  1 07:49:37 2019

@author: NISHANT
"""
def IVPMSNATURAL(Floodevent):
    import numpy as np
    import matplotlib.pyplot as plt
    from Evaluation_criteria import NashSf
    from Evaluation_criteria import ErPeak
    from Evaluation_criteria import EVOL
    from Evaluation_criteria import ApplicabilityCriteriaQ
    from Evaluation_criteria import TPER
    from naturalprop import propnatural

    #INFLOW HYDROGRAPH PARAMETERS

    import pandas as pd
    sheetn = input('Input Sheet Name: ')
    inflow = pd.read_excel('Tiberdata11.xlsx',sheet_name=sheetn)
    ibc=np.array(inflow.yuprism)
    lateral = pd.read_excel('Tiberdata11.xlsx',sheet_name = sheetn)
    ql=np.array(lateral.qlateral)
    benchmark = pd.read_excel('Tiberdata11.xlsx',sheet_name=sheetn)
    bmark = np.array(benchmark.ydprism)
    benchds=pd.read_excel('Tiberdata11.xlsx',sheet_name=sheetn)
    bds=np.array(benchds.Qd)
    inflowQ=pd.read_excel('Tiberdata11.xlsx',sheet_name=sheetn)
    QU = np.array(inflowQ.Qu)
    YDBM = pd.read_excel('Tiberdata11.xlsx',sheet_name=sheetn)
    YDBM = np.array(YDBM.ydact)
    Areau = pd.read_excel('Tiberdata11.xlsx',sheet_name=sheetn)
    AU = np.array(Areau.Au)
    Aread = pd.read_excel('Tiberdata11.xlsx',sheet_name=sheetn)
    AD = np.array(Aread.Ad)
    yuac=pd.read_excel('Tiberdata11.xlsx',sheet_name=sheetn)
    YUACT = np.array(yuac.yuact)
```

```
    # Areapr = pd.read_excel('Tiberdata.xlsx',sheet_name=sheetn)
    # Aprism = np.array(Areapr.Aprism)

    so,n,yi,tl,TD = propnatural(Floodevent)


    b = 35
    m = 2.805


    rl = 50 * 1000
    dx = 1*1000
    cs = int(round(rl/dx))+1

    dt =1800
    td = TD*3600 #total Duration inseconds

    t = np.arange(0,td,dt) # timeseries in seconds


    num = tl*60
    TL = num/50
    #-------------------------------------------------------------------------
-------------------------
                                    #Computational Interval
    #-------------------------------------------------------------------------
-------------------------


    #-------------------------------------------------------------------------
-------------------------
            #Finite Difference Grid Generation with Initial Condition and
Boundary Condition
    #-------------------------------------------------------------------------
-------------------------
    #Stage Routing Parameters
    Y = np.zeros((len(t),cs))
    QL = np.zeros((len(t),cs))
    Y[0,:]= yi #adding initial condition --Stage
    Y[:,0]= ibc # adding boundary condition --Stage
    for i in range(cs):
        QL[:, i] = ql
    k = np.zeros((len(t),cs))
    theta = np.zeros((len(t),cs))
```

```
    cel3 = np.zeros((len(t),cs))
    cel = np.zeros((len(t),cs))


    yo = Y[0,0]# Initial Depth

    #-----------------------------------------------------------------------
---------------------
        # Functions to calculate Various Parameters
    #-----------------------------------------------------------------------
---------------------
    def A(y): # function to calculate area
        area = (b + m*y)*y
        return area
    def P(y): # function to calculate Wetted Perimeter
        wettedperimeter = b + 2*y*np.sqrt(1+m**2)
        return wettedperimeter
    def V(y): # function to calculate velocity
        velocity = (1/n)*((A(y)/P(y))**(2/3))*np.sqrt(so)
        return velocity
    def B(y):# function to compute Top Width
        Topwidth = b + 2*y*m
        return Topwidth
    def dRdy(y):
        a = (P(y)*B(y) - A(y)*2*np.sqrt(1+m**2))/(P(y))**2
        return a
    def C(y):# function to calculate Celerity
        c = (1 + (2/3)*(P(y)/B(y))*dRdy(y))* V(y) #FOR VARIABLE C
        return c

    # B = np.zeros(len(t))
    # for i in range(len(t)):
    #     B = (Aprism[i+1]-Aprism[i])/(Y[i+1]-Y[i])
```

```
    Q=np.zeros((len(t),cs))
    Q[:,0] = QU


    #-----------------------------------------------------------------------
---------------------
        # Estimation of Initial K and Theta Corresponding to Initial
Steady Flow for stage Routing
    #-----------------------------------------------------------------------
---------------------
    # cel3[0,:] =  C(yo) #VARIABLE C
    # k[0,:] = dx/(C(yo)) #VARIABLE C


    c = dx/(TL)   #CONSTANT C
    cel[:,:] = c  #CONSTANT C

    #------------------------------FOR CONSTANT THETA--------------------
-----------------------------------------
    #def NewtonRaph(y,c): # y = initial guess (depth), Q =  discharge
        #def f(y):
            #function = c - ((1+((2/3)*(P(y)/B(y))*dRdy(y)))*V(y))
            #return function
        #def derivative(y):
            #h = 0.01
            #fprime = (f(y+h) - f(y))/h #fprime is derivative of f
            #return fprime
        #def iterate(y):
            #for i in range(50): # shouldn't we write x in range
                #x = y - (f(y)/derivative(y))
                #if (y == x): # it means if the value of x comes out to
be EQUAL TO y
                    #break
                #else:
                    #y = x  # it means that y IS x
            #return y
        #a =iterate(y)
        #return a
    #yav =  NewtonRaph(0.01,c)
    #-----------------------------------------------------------------------
-------------------------


    qo = A(yo)*V(yo)
    #qav = A(yav)*V(yav) #CONSTANT THETA

    # theta[0,:] = 0.5 - (qo / (2*so*B(yo)*C(yo)*dx)) # theta estimate of
initial time-step j = 0
```

```
    theta[0,:] = 0.5 - (qo / (2*so*B(yo)*c*dx)) # CONSTANT c
    #theta[:,:] = 0.5 - (qav / (2*so*B(yav)*c*dx)) #CONSTANT THETA
    Q[0,:]=qo



    for j in range(len(t)-1):
        for i in range(cs-1):

    #-------------------------------------------------------------------------
-----------------
                        # Stage Routing Begins Here
    #-------------------------------------------------------------------------
-----------------

            #step1: Estimation of Un-refined Flow depth at downstream
section

            Y[j+1,i+1]= Y[j,i+1] + Y[j+1,i]  - Y[j,i]

           #step2: depth at mid section i.e average of u/s depth and d/s
depth at same time level
            ym = 0.5 * (Y[j+1,i]+Y[j+1,i+1])

            #step3:finding q3, Q3 = QMO

            qm0 = A(ym)*V(ym) # QMO



            #step4: Compute theta at current time
            # theta[j+1,i+1] = 0.5 - (qm0/(2*so*B(ym)*C(ym)*dx))# Refined
Theta
            theta[j+1,i+1] = 0.5 - (qm0/(2*so*B(ym)*c*dx)) # Refined
Theta CONSTANT c
            #theta[j+1,i+1] = 0.5 - (qo / (2*so*B(yav)*c*dx)) #CONSTANT
THETA

            #step 7:Compute Average Cel  to compute k and compute
downstream depth

            y3 = Y[j+1,i+1] +   theta[j+1,i+1] *(Y[j+1,i] - Y[j+1,i+1]) #
Unsteady depth at sec-3
            v3 = qm0/A(y3)  # Unsteady velocity at sec-3
            # cel3[j+1,i+1] =  (1 + (2/3)*(P(y3)/B(y3))*dRdy(y3))* v3  #
Unsteady celerity at sec-3

            # cavg = 0.5 * (cel[j+1,i+1] + cel[j,i+1])#variable param
            # k[j+1,i+1] = dx/cavg
```

```
            k[j+1,i+1] = dx/c #CONSTANT C
            K = k[j+1,i+1]
            X =  0.5 * (theta[j+1,i+1] + theta[j,i+1] )


            #step 8 :Estimation of c1,c2,c3

            cd = K*(1-X)+0.5*dt

            c1 = (-K*X + 0.5 *dt)/cd
            c2 = (K*X + 0.5*dt)/cd
            c3 = (K*(1-X) - 0.5*dt)/cd
            c4 = (0.5*K*dt)/cd

            #step 9:Computation of  refined flow depth

            Y[j+1,i+1]= c1*Y[j+1,i]+ c2*Y[j,i]+
c3*(Y[j,i+1])+c4*((QL[j+1,i+1])+(QL[j,i+1]))*(1/B(y3))

            Yactd = np.zeros((len(t),cs))
            Yactd = (Y-0.0421)/1.149

            #Discharge hydrograph
           #Discharge hydrograph
            Ym = 0.5 * (Yactd[j+1,i]+Yactd[j+1,i+1]) #refinedYm
            qm0 = A(Ym)*V(Ym)#refined Q3
            # theta[j+1,i+1] = 0.5 - (qm0/(2*so*B(Ym)*C(Ym)*dx))#refined
theta(for varYing C)


            # theta[j+1,i+1] = 0.5 - (qo / (2*so*B(Yav)*c*dx))#CONSTANT
THETA

            # Y3 = Y[j+1,i+1] +   ((theta[j+1,i+1]) *(Y[j+1,i] -
Y[j+1,i+1]))#refined Y3
            # cel3[j+1,i+1] =  (1 + (2/3)*(P(Y3)/B(Y3))*dRdy(Y3))* v3 #
refined celeritY

            QM = qm0 * np.sqrt(1-(((Yactd[j+1,i+1])-
(Yactd[j+1,i]))/(so*dx)))

            # Q[j+1,i+1] = QM -  ((C(Ym))*B(Ym)*(Ym-Yactd[j+1,i+1]))
#variable param
            Q[j+1,i+1] = QM -  (c*B(Ym)*(Ym-Yactd[j+1,i+1]))#constant
param



    NSEYIVPMS = NashSf(Yactd[:,50],YDBM)
```

```
    yperIVPMS = ErPeak(Yactd[:,50],YDBM)
    typerIVPMS = TPER(Yactd[:,50],YDBM)



    #plt.savefig(' stage hyd 50 km 4 reaches trap 2.png')

    NSEQIVPMS = NashSf(Q[:,50],bds)
    QperIVPMS = ErPeak(Q[:,50],bds)
    ErVOLIVPMS = EVOL(Q[:,50],bds)
    tqperIVPMS = TPER(Q[:,50],bds)



    ivpmsnatural =
{"q50":Q[:,50],"NSEQIVPMS":NSEQIVPMS,"QperIVPMS":QperIVPMS,"ErVOLIVPMS":E
rVOLIVPMS,"tqperIVPMS":tqperIVPMS,"Y50":Y[:,50],"NSEY":NSEYIVPMS,"yperVPM
S":yperIVPMS,"typerVPMS":typerIVPMS,'YU':ibc,'Yactd':Yactd[:,50],'YDBM':Y
DBM,'YUACT':YUACT}

    fig,axes = plt.subplots(1,1,figsize = (10,4))
    axes.plot(t/3600,QU,'b',label='Inflow Discharge')# t vs Inflow
Discharge
    axes.plot(t/3600,Q[:,50],'r',label='Outflow Discharge')# t vs Outflow
Discharge
    axes.plot(t/3600,bds,'g',label = 'Benchmark Discharge')#t vs
Benchmark Discharge

axes.text(0.1,0.6,r'$\eta_{QIVPMS}$'+str(round(NSEQIVPMS,3)),transform=ax
es.transAxes, fontsize = 11)

axes.text(0.1,0.5,'q$_{perIVPMS}$'+str(round(QperIVPMS,3)),transform=axes
.transAxes, fontsize = 11)

axes.text(0.1,0.4,'EVOL$_{IVPMS}$'+str(round(ErVOLIVPMS,3)),transform=axe
s.transAxes, fontsize = 11)
    axes.set_title(input('Title name: '))
    axes.set_ylabel('Discharge(cumecs)')
    axes.set_xlabel('Time(h)')
    axes.legend(loc=0)

    fig,axes = plt.subplots(1,1,figsize = (10,4))
    axes.plot(t/3600,ibc,'b',label='Inflow Stage')# t vs Inflow Stage
    # axes.plot(t/3600,bmark, 'g',label='Benchmark Stage')# t vs
Benchmark Stage
    axes.plot(t/3600,YDBM, 'g',label='Benchmark Stage')
    #axes.plot(t/3600,Y[:,50],'m',label='Outflow Stage')# t vs Outflow
Stage
    axes.plot(t/3600,Yactd[:,50],'k',label='Outflow Stage')
```

```
    axes.text(0.1,0.6,r'$\eta_{yIVPMS}$'  +
str(round(NSEYIVPMS,3)),transform=axes.transAxes, fontsize = 11)
    axes.text(0.1,0.5,'y$_{perIVPMS}$'  +
str(round(yperIVPMS,3)),transform=axes.transAxes, fontsize = 11)
    axes.set_title(input('Title name: '))
    axes.set_ylabel('Stage(m)')
    axes.set_xlabel('Time(h)')
    axes.legend(loc=0)

    return ivpmsnatural
```

Appendix B

Python Code for RCM

```
# -*- coding: utf-8 -*-
"""
Created on Fri Jun  7 10:12:33 2019

@author: general
"""


# -*- coding: utf-8 -*-
"""
Created on Wed Mar 27 15:15:43 2019

@author: NISHANT
"""

# -*- coding: utf-8 -*-
"""
Created on Thu Mar 14 16:01:11 2019

@author: NISHANT
"""
def RCMnatural(Floodevent):
    import numpy as np
    import matplotlib.pyplot as plt
    from Evaluation_criteria import NashSf
    from Evaluation_criteria import ErPeak
    import pandas as pd
    from Evaluation_criteria import EVOL
    from Evaluation_criteria import TPER
    from naturalprop import propnatural



    sheetn = input('Input sheet name: ')

    inflow=pd.read_excel("Tiberdata11.xlsx",sheet_name= sheetn)
    QU=np.array(inflow.Qu)
    lateral = pd.read_excel("Tiberdata11.xlsx",sheet_name = sheetn)
    ql=np.array(lateral.qlateral)
    Areau=pd.read_excel("Tiberdata11.xlsx",sheet_name=sheetn)
    AU=np.array(Areau.Au)
    Aread=pd.read_excel("Tiberdata11.xlsx",sheet_name=sheetn)
    AD=np.array(Aread.Ad)
```

```
Qbmark=pd.read_excel("Tiberdata11.xlsx",sheet_name=sheetn)
QBM=np.array(Qbmark.Qd)
yd=pd.read_excel("Tiberdata11.xlsx",sheet_name = sheetn)
YD=np.array(yd.ydprism)
D = np.zeros(len(QU))

so,n,yi,tl,TD = propnatural(Floodevent)

dt = 1800
td = TD*3600
t = np.arange(0,td,dt)
QD=np.zeros((len(t)))
L=50000 # Length of reach = 50 km

B = 35 # channel width = 15m


def tb(YD):
    for i in range(len(YD)):
        if YD[i+1]-YD[i] != 0:
            break
    return i

num = tl
TL=int(num/15) # TL = Time Shift
tL = num*60
TB=tb(YD) # TB = Time when the rising limb starts
TP=np.argmax(YD) # TP index = time to peak of downstream stage
hydrograph
TP1=np.argmax(QU)
delt=int(TP1/5) #delt* index
TP1abs = t[TP1] # TP value
deltabs = int(TP1abs/5) # delt* value
TPBM = np.argmax(QBM)

qp=(AD[TP]-AU[TP-TL])/(tL) # lateral flow contribution


#Qd(tb) determination
u =( QU[TB-TL])/(AU[TB-TL])
QD[TB]=u*AD[TB]

#Q* determination
R = L/((2*B*so)*(L/tL)**3)

S = QU[TP]

tp1 = TP1+delt
tp2 = TP1-delt
```

```
    T = abs(((QU[tp1])+(QU[tp2])-(2*(QU[TP1])))/((deltabs)**2))

    Qatt=R*S*T

    #Qd(tp)determination
    QD[TP]=QU[TP-TL] + (qp*L) #w/o attenuation param
    # QD[TP]=QU[TP-TL] + (qp*L) - Qatt # with attenuation param

    #alpha and beta

    A=QD[TP]-QD[TB]
    B = ((AD[TP])*(QU[TP-TL]))/(AU[TP-TL])
    C = ((AD[TB])*(QU[TB-TL]))/(AU[TB-TL])

    alpha = A/(B-C)
    # alpha = 1.1105


    M=QD[TB]
    N=(alpha*(AD[TB])*(QU[TB-TL]))/(AU[TB-TL])

    beta=M-N
    # beta = -2.149


    #Qd(t) (outflow Discharge)

    for i in range(len(QU)):
        QD[i]=(alpha*(AD[i])*(QU[i-TL]))/(AU[i-TL]) + beta


        D[i] = ((AD[i])*(QU[i-TL]))/(AU[i-TL])

    NSER = NashSf(QD,QBM) # NSE of RCM
    Qper = ErPeak(QD,QBM) # Error in peak discharge of RCM
    ErVOLRCM = EVOL(QD,QBM) # Percentage error in volume conservation of
RCM
    tpqerRCM = TPER(QD,QBM) # Time to peak reproduction of RCM


    RCMnatural =
{"QD":QD,"QU":QU,"NSEQRCM":NSER,"QperRCM":Qper,"ErVOLRCM":ErVOLRCM,"tpqer
RCM":tpqerRCM,"QBM":QBM,'alpha':alpha,'beta':beta,'Qatt':Qatt}



    fig,axes = plt.subplots(1,1,figsize = (10,4))
    titlen = input('Title name: ')
```

```
    axes.set_title('RCM and IVPMS' +  str(titlen))
    axes.plot(t/3600,QU,'b',label='Inflow Discharge')# t vs I
    axes.plot(t/3600,QD,'r',label='RCM') # t vs RCM outflow discharge
    axes.plot(t/3600,QBM,'g',label='BMARK') # t vs Benchmark outflow
discharge
    # axes.plot(t/3600,Q[:,50],'k',label='IVPMS') # t vs IVPMS outflow
discharge
    axes.text(0.1,0.9,r'$\eta_{RCM}$'  +
str(round(NSER,3)),transform=axes.transAxes, fontsize = 11)
    axes.text(0.1,0.8,'Q$_{perRCM}$'+
str(round(Qper,3)),transform=axes.transAxes,fontsize = 11)
    axes.text(0.1,0.7,'EVOL$_{RCM}$' +
str(round(ErVOLRCM,3)),transform=axes.transAxes,fontsize = 11)
    # axes.text(0.6,0.9,r'$\eta_{IVPMS}$'  +
str(round(NSEQIVPMS,3)),transform=axes.transAxes, fontsize = 11)
    # axes.text(0.6,0.8,'Q$_{perIVPMS}$'+
str(round(QperIVPMS,3)),transform=axes.transAxes,fontsize = 11)
    # axes.text(0.6,0.7,'EVOL$_{IVPMS}$' +
str(round(ErVOLIVPMS,3)),transform=axes.transAxes,fontsize = 11)

    axes.set_ylabel('Discharge(cumecs)')
    axes.set_xlabel('Time(h)')

    axes.legend(loc=0)
    plt.savefig('IVPMS & RCM' + str(titlen))

    return RCMnatural
```